AN ABSTRACT OF THE THESIS OF

F. Bryan Grigsby for the degree of Master of Science in Geology presented on January 14, 1986.

Title: Quaternary Tectonics of the Rincon and San Miguelito Oil Fields Area, Western Ventura Basin, California

Redacted for Privacy

Abstract approved: Dr. Robert S. Yeats

The Ventura basin is an elongate sedimentary trough extending from the San Gabriel fault west into the Santa Barbara Channel. West of Ventura it contains over 4 km of severely deformed Pliocene and Pleistocene clastic strata. The north-dipping Red Mountain reverse fault system, which forms the northern boundary of the basin, has been active since the early Pliocene and has maximum reverse separation of 7300 m (23,900 ft). In the basin, the Grubb and Oak Grove faults were active in the early Pleistocene and were reactivated during late Pleistocene folding. Both are tear faults that dip steeply northeast and strike northwest, in contrast to the west-trending structural grain of the region. The Rincon anticline is the western extension of the Ventura Avenue anticline. Both anticlines formed approximately 200,000 years ago as rootless folds which die out in subjacent fine-grained Miocene strata. Above the Rincon anticline synchronous

shortening occurred on the Javon Canyon/Padre Juan fault and San Miguelito anticline. The Padre Juan fault is a south-dipping reverse fault that flattens over the axis of the Rincon anticline and dies out to the north. Where it flattens, the Javon Canyon fault rises upwards and offsets 3500 year old marine terrace deposits at the surface. Maximum reverse separation across the Javon Canyon/Padre Juan fault is 2800 m (9200 ft). The steeply north-dipping to overfolded region between the Javon Canyon and Padre Juan faults constitutes a large portion of the north limb of the San Miguelito anticline. This anticline, constrained above the Padre Juan fault, is a complex example of a fault-propagation fold. Total shortening in the Ventura basin along a cross-section through the study area is approximately 7825 m (25,700 ft). For the last 200,000 years this north-south directed shortening has occurred at a rate of 12.5 to 22.3 mm/yr (0.49 to 0.87 in/yr). These values compare favorably with shortening values obtained at other locations in the basin, and support the concept of decreasing horizontal contraction from east to west across the basin for the last 200,000 years.

Quaternary Tectonics of the
Rincon and San Miguelito Oil Fields Area,
Western Ventura Basin, California

by

F. Bryan Grigsby

A THESIS

submitted to

Oregon State University

in partial fulfillment of
the requirements for the
degree of

Master of Science

Completed January 14, 1986

Commencement June 1986

APPROVED:

Redacted for Privacy

Professor of Geology in charge of major

Redacted for Privacy

Head of department of Geology

Redacted for Privacy

Dean of Graduate School

Date thesis is presented January 14, 1986

ACKNOWLEDGMENTS

Support was provided by U. S. Geological Survey Earthquake Hazards Reduction Program Grant No. 14-08-0001-19173 awarded to R. S. Yeats, and by direct financial assistance from Conoco, Inc. and Santa Fe Energy Company. Additional assistance was provided by Mobil Oil Corporation. R. S. Yeats of Oregon State University shared freely his comprehensive knowledge of the geology of the Ventura basin and critically reviewed this work. Lu Huafu of Nanjing University, Nanjing, China assisted in the early part of the study. R. O. Beringer and R. Hubbell of Conoco, Inc. gave critical advice and support. T. W. Dibblee, Jr. and A. M. Sarna-Wojcicki of the U. S. Geological Survey provided unpublished surface geologic maps of the area.

Over the course of this investigation, the camaraderie of my fellow Dawes House residents was greatly appreciated, as was the time spent with Matt Richards discussing the geology of California. Anne's assistance, concern, and patience were indispensable to my seeing this project through to its end.

TABLE OF CONTENTS

INTRODUCTION	1
REGIONAL GEOLOGIC SETTING	14
Pre-Pliocene Geology	14
Plio-Pleistocene Geology	25
Surficial Deposits and Landslides	30
QUATERNARY STRUCTURES	32
Red Mountain Fault System	32
Early Pleistocene Ventura Basin Structures	41
Late Pleistocene Folding and Faulting	49
San Miguelito Anticline, Rincon Anticline, and Associated Structures	49
Javon Canyon/Padre Juan Fault	56
Minor South-dipping Reverse Faults	60
KINEMATIC ANALYSIS OF LATE PLEISTOCENE TO RECENT DEFORMATION	63
Late Pleistocene Folding	63
Javon Canyon/Padre Juan Faulting and San Miguelito Anticline Folding	70
Late Pleistocene Shortening Due to Red Mountain Faulting and Folding	76
CONCLUSIONS	82
REFERENCES CITED	91
APPENDIX I, Complete List of Wells Used in Study	96
APPENDIX II, Plates I-XVII	Pocket

LIST OF FIGURES

Figure		Page
1	Regional tectonic map of western Transverse Ranges, California	2
2	Index map of Rincon, San Miguelito, and western Ventura Avenue oil fields area	6
3	Geologic map of Rincon, San Miguelito, and western Ventura Avenue oil fields area	8
4	Stratigraphy of northern Ventura basin	15
5A-5G	Cross-sections A-A', C-C', F-F', J-J', K-K', M-M', and P-P'	17-24
6	Fault contour map	33
7	Cross-section J-K': Present, and restored to pre-deformation condition	37
8	Map of surface and shallow subsurface structural elements	44
9	Structure contour map of "Jc" horizon	46
10	Photo and line drawing of San Miguelito anticline in west face of San Miguelito amphitheater	50
11	Fault-bend fold and fault-propagation fold comparison	72
12	Regional cross-section II	80

LIST OF TABLES

Table		Page
1	Key to wells used in text	10
2	Magnitudes and rates of Plio-Pleistocene shortening along cross-section J-K' and cross-section II	68
3	Comparison of Plio-Pleistocene shortening in the central and western Ventura basin	88

LIST OF PLATES

Plate		In pocket
I	Geologic map of Rincon, San Miguelito, and western Ventura Avenue oil fields area (1:24,000)	
II	Well base map and cross-section locations	
III	Composite type electric log	
IV	Structure contour map of "Jc" electric log marker	
V	Fault contour map of the Padre Juan fault	
VI	Fault contour map of the Grubb and Oak Grove faults showing their relation to the Javon Canyon/Padre Juan fault	
VII	Cross-sections A-A' and B-B'	
VIII	Cross-section C-C'	
IX	Cross-sections D-D' and E-E'	
X	Cross-sections F-F' and G-G'	
XI	Cross-sections H-H' and I-I'	
XII	Cross-section J-J'	
XIII	Cross-section K-K'	
XIV	Cross-sections L-L' and M-M'	
XV	Cross-sections N-N' and O-O'	
XVI	Cross-section P-P'	
XVII	Cross-section Q-Q'	

QUATERNARY TECTONICS OF THE RINCON AND SAN MIGUELITO OIL FIELDS AREA, WESTERN VENTURA BASIN, CALIFORNIA

INTRODUCTION

The west-trending Ventura basin is located in the western Transverse Ranges geomorphic province. The basin is bounded on the north by the Santa Ynez Mountains and the Topatopa Mountains, on the south by the northern Channel Islands and the Santa Monica Mountains, and on the east by the San Gabriel fault (Fig. 1). To the west, it extends the length of the Santa Barbara Channel to the edge of the continental shelf. Folded Tertiary and Cretaceous strata occur north of the fault-bounded northern margin of the basin and in the upthrown block south of the Oak Ridge fault. Miocene volcanics, Tertiary and Cretaceous strata, and crystalline basement are exposed in the northern Channel Islands and the Santa Monica Mountains. Precambrian crystalline basement bounds the basin to the east.

The Ventura basin formed during the Miocene, following the collision of the Pacific and North American plates and the subsequent migration of the Mendocino triple-junction north of the western Transverse Ranges. The west trend of Transverse Ranges structures is a result of the clockwise rotation of the region following the onset of transform faulting at the plate boundary

Figure 1: Regional tectonic map of western Transverse Ranges, California. Cross-sections I, III, and IV represent locations where Yeats (1981) calculated convergence rates across the Ventura basin. Cross-section II, shown in Figure 12, is the location where convergence rates were calculated in this study. ACS, Ayers Creek Syncline; CLS, Cañada Larga syncline; JC/PJF, Javon Canyon/Padre Juan fault; RMA, Red Mountain anticline; VAA, Ventura Avenue anticline.

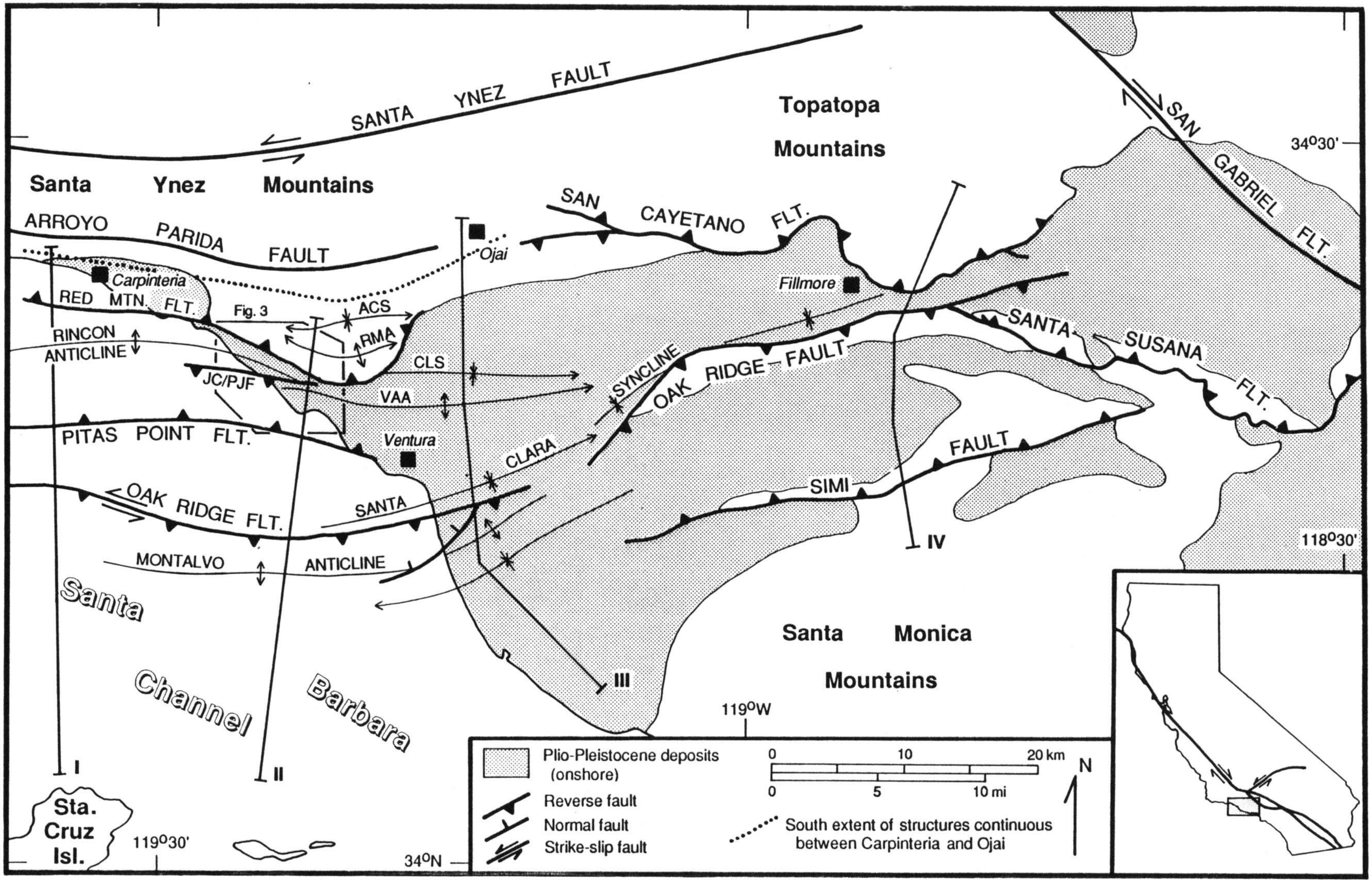
SANTA YNEZ FAULT
Topatopa Mountains
SAN GABRIEL FLT.
34°30'
Santa Ynez Mountains
ARROYO PARIDA FAULT
SAN CAYETANO FLT.
Ojai
Carpinteria
RED MTN. FLT.
Fig. 3
ACS
RMA
Fillmore
SANTA SUSANA FLT.
RINCON ANTICLINE
CLS
SYNCLINE
OAK RIDGE FAULT
JC/PJF
VAA
PITAS POINT FLT.
Ventura
CLARA
FAULT
SIMI
OAK RIDGE FLT.
SANTA
IV
118°30'
MONTALVO ANTICLINE
Santa Barbara Channel
Santa Monica Mountains
III
119°W
I
II
Sta. Cruz Isl.
119°30'
34°N
Plio-Pleistocene deposits (onshore)
Reverse fault
Normal fault
Strike-slip fault
0 10 20 km
0 5 10 mi
N
South extent of structures continuous between Carpinteria and Ojai

Figure 1.

(Luyendyk et al, 1980). South of Fillmore, within the Ventura basin, 7000 m (23,000 ft) of Plio-Pleistocene marine and nonmarine clastic strata occur, the thickest sequence of this age known in the world. Many structural and stratigraphic traps in these strata are oil and gas bearing; consequently, thousands of wells have been drilled in the basin. A rich foraminiferal fauna provides biostratigraphic control for much of the basin. Absolute age control is provided by magnetic-reversal stratigraphy, by volcanic ash tephrochronology, and by uranium-series, radiocarbon, and amino-acid racemization dating methods applied to uplifted marine terrace deposits.

Uplift and horizontal contraction characterize the present tectonic style in the western Transverse Ranges. In northern Ventura basin crustal shortening has been identified at three levels: 1) along the basin boundary where the Red Mountain reverse fault system extends downward into high-strength basement rocks; 2) within fine-grained Miocene strata in the basin where the Ventura Avenue anticline dies out, possibly along a major zone of detachment; and 3) within the Plio-Pleistocene sequence in the basin where reverse faults contained within west-trending anticlines ramp upwards from siltstone interbeds. This study examines the morphology and kinematics of the Pliocene to Holocene structures, many similar to those mentioned above, found in the laterally shortened basin sequence directly south of, and including, the north-dipping Red Mountain reverse fault system.

The study area is bounded roughly by the Red Mountain anticline on the north, the Santa Barbara Channel on the south and west, and Cañada del Diablo on the east (Figs. 2, 3). The investigation involved primarily the analysis of subsurface data obtained from oil wells drilled in and adjacent to Rincon and San Miguelito oil fields. To work out the three-dimensional structural geology of the region, electric logs, dipmeter logs, well histories, directional surveys, and paleontologic and core reports were used to construct geological cross-sections and structure contour and fault isoseparation maps. Data for the more than 400 oil wells chosen for study (Table 1, Appendix I) were acquired from oil operators and from the California Division of Oil and Gas. The subsurface interpretations were incorporated in compiling the surface geologic map (Plate I, simplified as Fig. 3). This map draws heavily on prior maps by Putnam (1942), Dibblee (unpubl. mapping 1938 through 1980), Weber et al (1973), Jackson (1981), Sarna-Wojcicki et al (1979, and in press), Sarna-Wojcicki (unpubl. mapping), and on unpublished oil industry maps.

Figure 2: Index map of Rincon, San Miguelito, and western Ventura Avenue oil fields area, California, showing cross-sections referred to in text. Modified from Pitas Point, California and Ventura, California 7 1/2 minute U. S. Geological Survey topographic quadrangle maps. Oil field limits from Weber et al (1973). J-K' is cross-section referred to in text. Numbered wells are those drilled outside oil field boundaries; see Table 1.

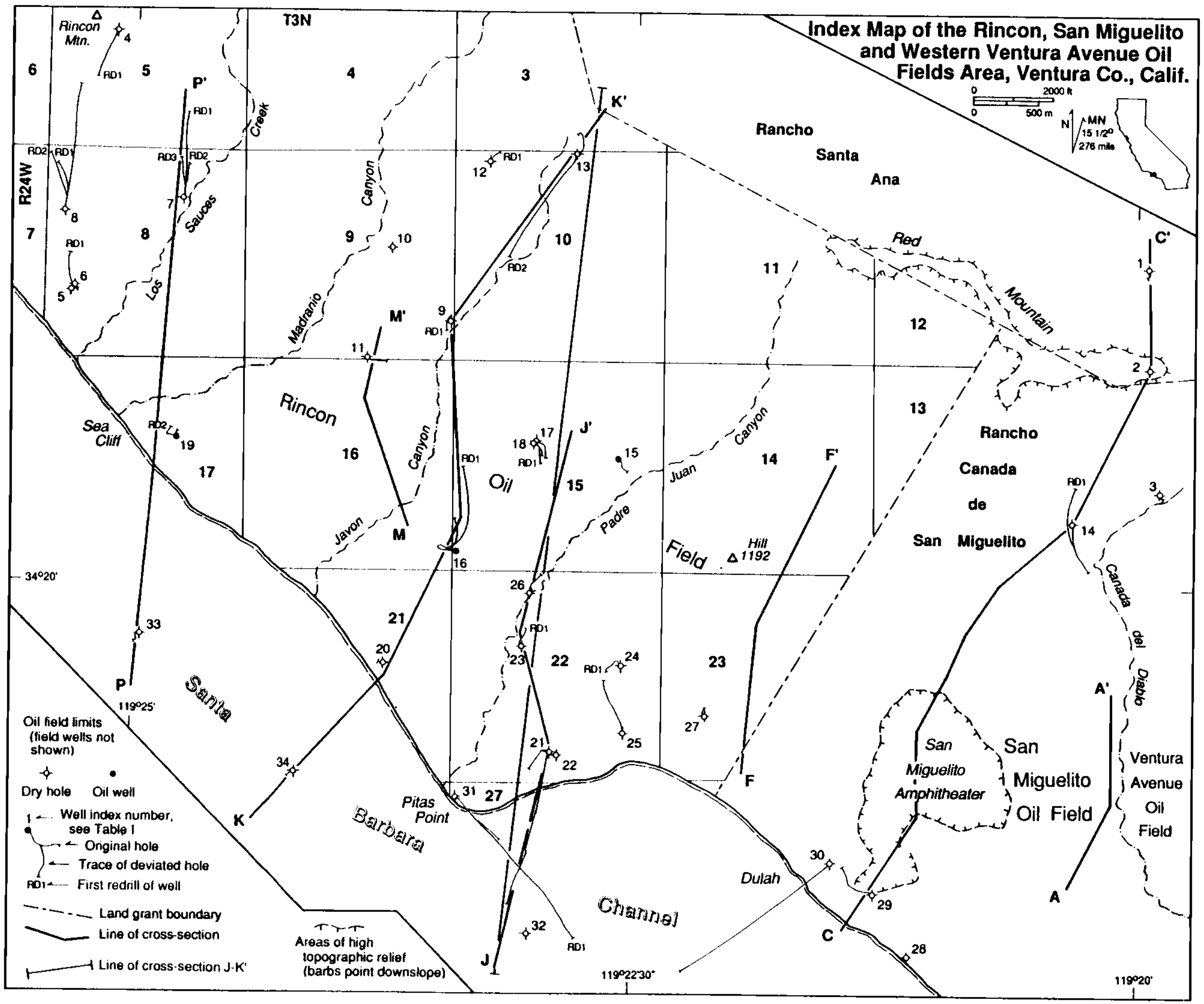
Index Map of the Rincon, San Miguelito and Western Ventura Avenue Oil Fields Area, Ventura Co., Calif.
Rincon Mtn.
T3N
R24W
Rancho Santa Ana
Rancho Canada de San Miguelito
Rincon Oil Field
San Miguelito Amphitheater
San Miguelito Oil Field
Ventura Avenue Oil Field
Santa Barbara Channel
Pitas Point
Sea Cliff
Dulah
Red Mountain
Hill 1192
Los Sauces Creek
Madranio Canyon
Javon Canyon
Padre Juan Canyon
Canada del Diablo
34°20'
119°25'
119°22'30"
119°20'
Oil field limits (field wells not shown)
Dry hole
Oil well
Well index number, see Table I
Original hole
Trace of deviated hole
First redrill of well
Land grant boundary
Line of cross-section
Line of cross-section J-K'
Areas of high topographic relief (barbs point downslope)

Figure 2.

Figure 3: Geologic map of Rincon, San Miguelito, and western Ventura Avenue oil fields area, California. Compiled and modified from Dibblee (unpubl. mapping 1938-1980); Weber et al (1973); Jackson (1981); Sarna-Wojcicki et al (1984, in press); Sarna-Wojcicki (unpubl. mapping); and from unpublished oil industry maps. JC/PJF, Javon Canyon/Padre Juan fault; RMF, Red Mountain fault. ka = years x 10^3.


Geologic Map of the Rincon, San Miguelito and Western Ventura Avenue Oil Fields Area, Ventura Co., Calif.
0 2000 ft
0 500 m
N
MN
15 1/2°
276 mils
From Pitas Point, California and Ventura, California U. S. Geological Survey 7 1/2' topographic quadrangle maps.
LEGEND FOR GEOLOGIC MAP AND CROSS-SECTIONS
Qls Landslides
Qu Undiff. alluvial deposits
Qt Terraces: Qt1-Punta Gorda (60-40 ka); Qt2-Sea Cliff (5.8-1.8 ka)
Qoa Older alluvium
Qsg Saugus Fm.
Qsb Santa Barbara Fm.
QTp Pico Fm.: QTpl-"lower"; QTpm-"middle"; QTpu-"upper"
Tpr Repetto Fm.
Tsq Sisquoc Fm.
Tm Monterey Fm.
Tr Rincon Fm.
Tv Vaqueros Fm.
Ts Sespe Fm.
Tcw Coldwater Fm.
Tcd-Tma Cozy Dell-Matilija Fms. (undiff.)
Attitude of bedding
Overturned bedding
Vertical beds
Volcanic Ash
GM-D: Glass Mountain-D Ash (0.8-0.9 Ma)
Ba: Bailey Ash (1.2 Ma)
Formation contact dashed where inferred
Fault contact dashed where inferred dotted where covered U-up D-down arrow shows direction of dip
Anticline arrow indicates direction of plunge
Syncline arrow indicates direction of plunge
Line of cross-section
RINCON
Sea Cliff
Pitas Point
Dulah
LOS SAUCES CREEK ANTICLINE
RED MOUNTAIN ANTICLINE
RED MTN. FLT.
RMF (NORTH 2)
RMF (MAIN)
RMF (SOUTH 2)
RINCON ANTICLINE
NORTH SYNCLINE
JAVON CANYON FLT.
JC/PJF
SAN MIGUELITO ANTICLINE
VENTURA AVENUE ANTICLINE
D-S FLT.
119°25'
34°20'
119°22'30"
119°20'
710 m
670 m
50 m

Figure 3.

Table 1: Key to wells used in text. A) Guide to numbered wells shown in Figure 2. Elevations and depths are given in feet. DF, drill floor; KB, Kelly bushing; OH, original hole; RD, redrill (RD1 is first redrill, RD2 is second redrill, etc.); RT, rotary table. B) Guide to field well abbreviations.

TABLE 1-A: GUIDE TO NUMBERED WELLS SHOWN IN FIGURE 2

Map No.	Well Operator	Well Name	Elevation	Depth
		T3N - R24W		
4	McCarthy Oil & Gas	Hobson 1	1971 KB	5515 OH 5650 RD1
5	Bond Development Corp.	Rincon 1	573 KB	5485
6	Shell	Tomson 1	577 DF	9704 OH 8670 RD1
7	Union	Un.-Std.-Hob. A-1	272 RT	6073 OH 9500 RD1 7565 RD2 6685 RD3
8	Union	Un.-Std.-Hob. B-1	711 RT	11020 OH 8958 RD1 7353 RD2
9	Amerada Hess	H & S 1	497 KB	4514 OH 6615 RD1
10	Kellerman	Vigus 1		2300
11	Ridge Oil	Fox 1	540 DF	8000
12	Amerada Hess	R. C. 1	1652 KB	4065 OH 2715 RD1
13	Shell	Hoffman Trust 1-10	1462 KB	11879 OH 13790 RD2
15	Conoco	Hobson 3	565 KB	7210
16	Conoco	Mobil-Padre 1	711 KB	14100 OH 15190 RD1
17	Mobil	Smith-Hobson 70	596 KB	11500
18	Shell	Hobson-Smith 2-1	591 DF	6275 OH 6144 RD1
19	Santa Fe	Hobson C-10A	35 DF	10002 OH 11650 RD2
20	Arco	Smith-Hoffman 1	55 KB	8107
21	Chevron	St. 3403-1	47 KB	17000
22	Chevron	S. P. Pitas Point 1	47 KB	9695
23	Conoco	CCMO-Hobson A-1	296 KB	8648 OH 7240 RD1
24	Petrominerals	CWOD-Faria 1	120 KB	7070 RD1
25	Santa Fe	Faria 1	50 KB	14717
26	Santa Fe	Hobson A-1	222	6970
27	Getty	Valenzuela 1	374	7828
31	Union	Santa Barbara C. H. 13	22 RT	7086

TABLE 1-A (CONT.)

Rancho Santa Ana Land Grant

1	Conoco	Casitas 1		8018
2	Conoco	Casitas 2		12188

Rancho Cañada de San Miguelito Land Grant

3	Shell	Wood 1		5745
14	Conoco	Grubb 173	937 KB	11388 OH 12107 RD1
28	Chevron	Solimar S. P. C. H. 1	33 DF	6469
29	Conoco	Grubb 94	88 KB	11227
30	Pauley Petroleum	C. H. 8-26-3A	32 KB	7724

Offshore

32	Chevron	C. H. 8R-49	17 KB	4519
33	Pauley Petroleum	C. H. 8-22-1A	12 KB	5520
34	Pauley Petroleum	C. H. 8-22-2A	20 KB	4508

TABLE 1-B: GUIDE TO FIELD WELL ABBREVIATIONS

A-___: Santa Fe Energy Corp., Hobson-A lease Rincon oil field wells.

B-___: Santa Fe Energy Corp., Hobson-B lease Rincon oil field wells.

C-___: Santa Fe Energy Corp., Hobson-C lease Rincon oil field wells.

OG-___: Santa Fe Energy Corp., Oak Grove lease Rincon oil field wells.

P-___: Mobil Oil Co., Padre lease Rincon oil field wells.

G-___: Conoco Inc., Grubb lease San Miguelito oil field wells.

T-___: Shell Oil Co., Taylor lease Ventura Avenue oil field wells.

REGIONAL GEOLOGIC SETTING

Pre-Pliocene Geology

Latest Eocene and Oligocene nonmarine Sespe Formation, and the overlying marine Vaqueros, Rincon, Monterey, and Sisquoc Formations of latest Oligocene to early Pliocene age crop out in the study area north of the Red Mountain fault (Figs. 3, 4). The Sespe is underlain by marine Eocene strata, penetrated by wells 1 and 2 (Figs. 2, 5B) in the core of the doubly plunging Red Mountain anticline. Northwest of the study area, the Eocene and Oligocene sequence consists of more that 300 m (1000 ft) of Matilija Sandstone, 600 to 820 m (1970 to 2690 ft) of Cozy Dell Formation, 820 m (2690 ft) of Coldwater Sandstone, and 1370 to 1600 m (4500 to 5250 ft) of Sespe Formation (Fig. 4; Dibblee, 1966; Jackson and Yeats, 1982). At Red Mountain, the Sespe Formation is only 1160 m (3800 ft) thick and the underlying Coldwater Sandstone only 550 m (1800 ft) thick. Beneath them is at least 1000 m (3300 ft) of undifferentiated Cozy Dell-Matilija strata (Fig. 5B). These rocks and the overlying 115 to 150 m (380 to 500 ft) veneer of Vaqueros Formation sandstone are moderately-indurated to well-indurated arkosic fine-grained to conglomeratic clastic rocks of relatively high mechanical strength.

Overlying this structurally competent sequence are

Figure 4: Stratigraphy for the northern Ventura basin area between Ventura and Santa Barbara, including subsurface stratigraphy for the Plio-Pleistocene strata encountered at the Rincon and San Miguelito oil fields. Volcanic ash bed abbreviations: Ba, Bailey; GM-D, Mono-Glass Mountain D; LC, Lava Creek. See Sarna-Wojcicki et al (1984) for discussion of ash bed age determinations. 1) Benthic foraminiferal faunal stages of Natland (1952). 2) Pico Formation markers are those used by industry workers in Rincon oil field; Repetto Formation markers are those used in San Miguelito oil field. "Jc" marker is equivalent to "AO" marker used at Ventura Avenue oil field (cf. Hsü, 1977; Yeats, 1979; 1983). 3) Amino-acid racemization age determined for <u>Protothaca</u> mollusk shells in youngest preserved Saugus Formation (Lajoie et al, 1979; 1982). 4) Regional correlation horizons used by Yeats (1981), based on lithology and benthic foraminifera biostratigraphy; ∴5 is a 1.0 Ma chronostratigraphic horizon.

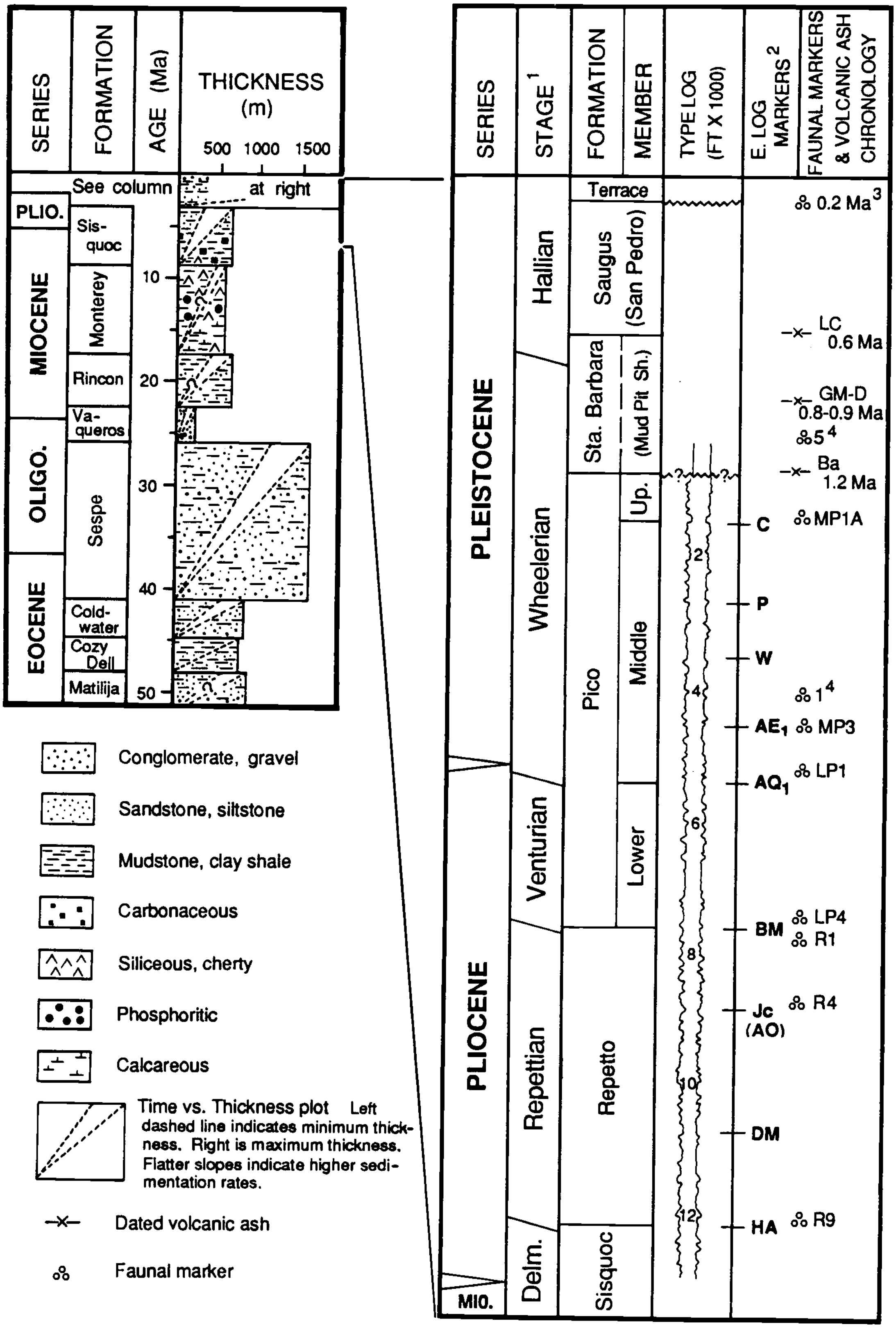
SERIES
FORMATION
AGE (Ma)
THICKNESS (m)
500 1000 1500
See column at right
PLIO.
MIOCENE
OLIGO.
EOCENE
Sis-quoc
Monterey
Rincon
Va-queros
Sespe
Cold-water
Cozy Dell
Matilija
10
20
30
40
50
Conglomerate, gravel
Sandstone, siltstone
Mudstone, clay shale
Carbonaceous
Siliceous, cherty
Phosphoritic
Calcareous
Time vs. Thickness plot Left dashed line indicates minimum thickness. Right is maximum thickness. Flatter slopes indicate higher sedimentation rates.
Dated volcanic ash
Faunal marker
SERIES
STAGE 1
FORMATION
MEMBER
TYPE LOG (FT X 1000)
E. LOG MARKERS 2
FAUNAL MARKERS & VOLCANIC ASH CHRONOLOGY
PLEISTOCENE
PLIOCENE
MIO.
Hallian
Wheelerian
Venturian
Repettian
Delm.
Terrace
Saugus (San Pedro)
Sta. Barbara (Mud Pit Sh.)
Pico
Up.
Middle
Lower
Repetto
Sisquoc
2
4
6
8
10
12
C
P
W
AE1
AQ1
BM
Jc (AO)
DM
HA
0.2 Ma 3
LC 0.6 Ma
GM-D 0.8-0.9 Ma
5 4
Ba 1.2 Ma
MP1A
1 4
MP3
LP1
LP4
R1
R4
R9

Figure 4.

Figure 5A-5G: Cross-sections A-A', C-C', F-F', J-J', K-K', M-M', and P-P'. No vertical exaggeration. Location of cross-section lines shown in Figures 2 and 3. Formation abbreviations shown on geologic map (Fig. 3). For well names see Table 1. Z, Zemorrian; S, Saucesian; Rel, Relizian; L, Luisian; Mo, Mohnian; and D, Delmontian are microfaunal Stages of Kleinpell (1938). R, Repetto; LP, "lower" Pico; MP, "middle" Pico; and UP, "upper" Pico are oil industry microfaunal intervals (R corresponds approximately with the Repettian microfaunal Stage of Natland (1952); LP with the Venturian Stage; MP with the lower Wheelerian Stage; and UP with the upper Wheelerian and lower Hallian Stages). For these intervals, the higher the subinterval number the deeper in the section the subinterval. A, away; Ba, Bailey ash; Bar, barren; BOSB, "base of steep beds"; JCF, Javon Canyon fault; Mio, Miocene; NS, North syncline; RA, Rincon anticline; RMA, Red Mountain anticline; RMF, Red Mountain fault; RS, Rincon syncline; SMA, San Miguelito anticline; T, towards; TOSB, "top of steep beds"; VAA, Ventura Avenue anticline.

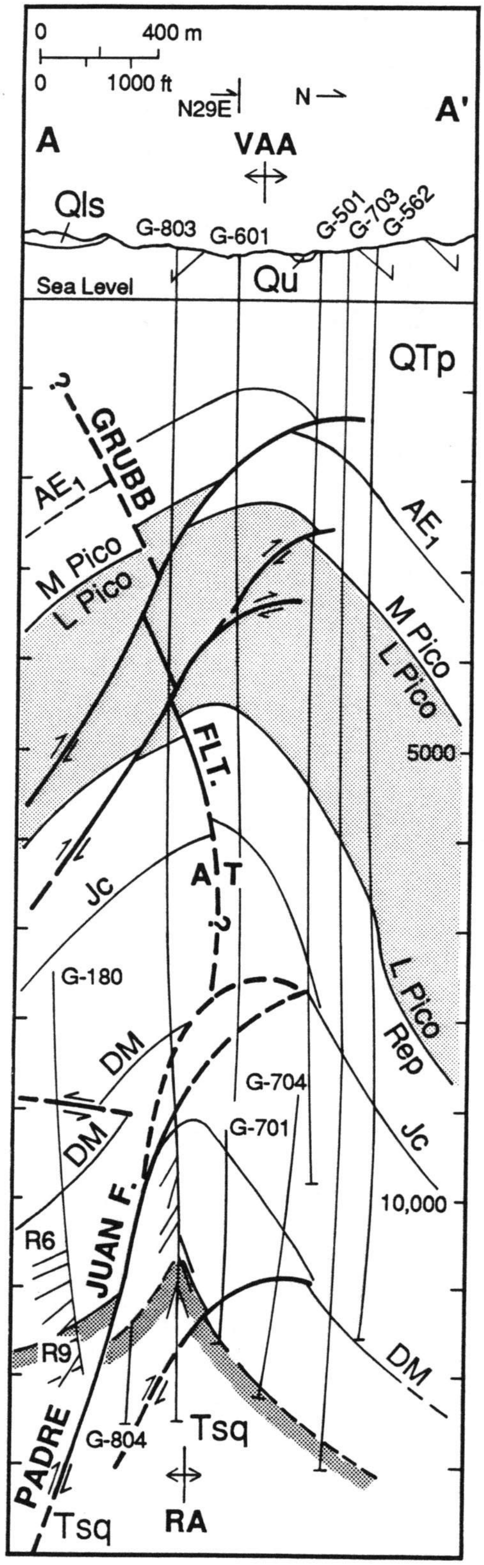
0 400 m
0 1000 ft
N29E
N
A
A'
VAA
Qls
G-803
G-601
G-501
G-703
G-562
Sea Level
Qu
QTp
GRUBB
AE1
M Pico
L Pico
FLT.
5000
A T
Jc
G-180
DM
L Pico
Rep
G-704
G-701
Jc
10,000
JUAN F.
R6
R9
DM
PADRE
G-804
Tsq
Tsq
RA

Figure 5A.

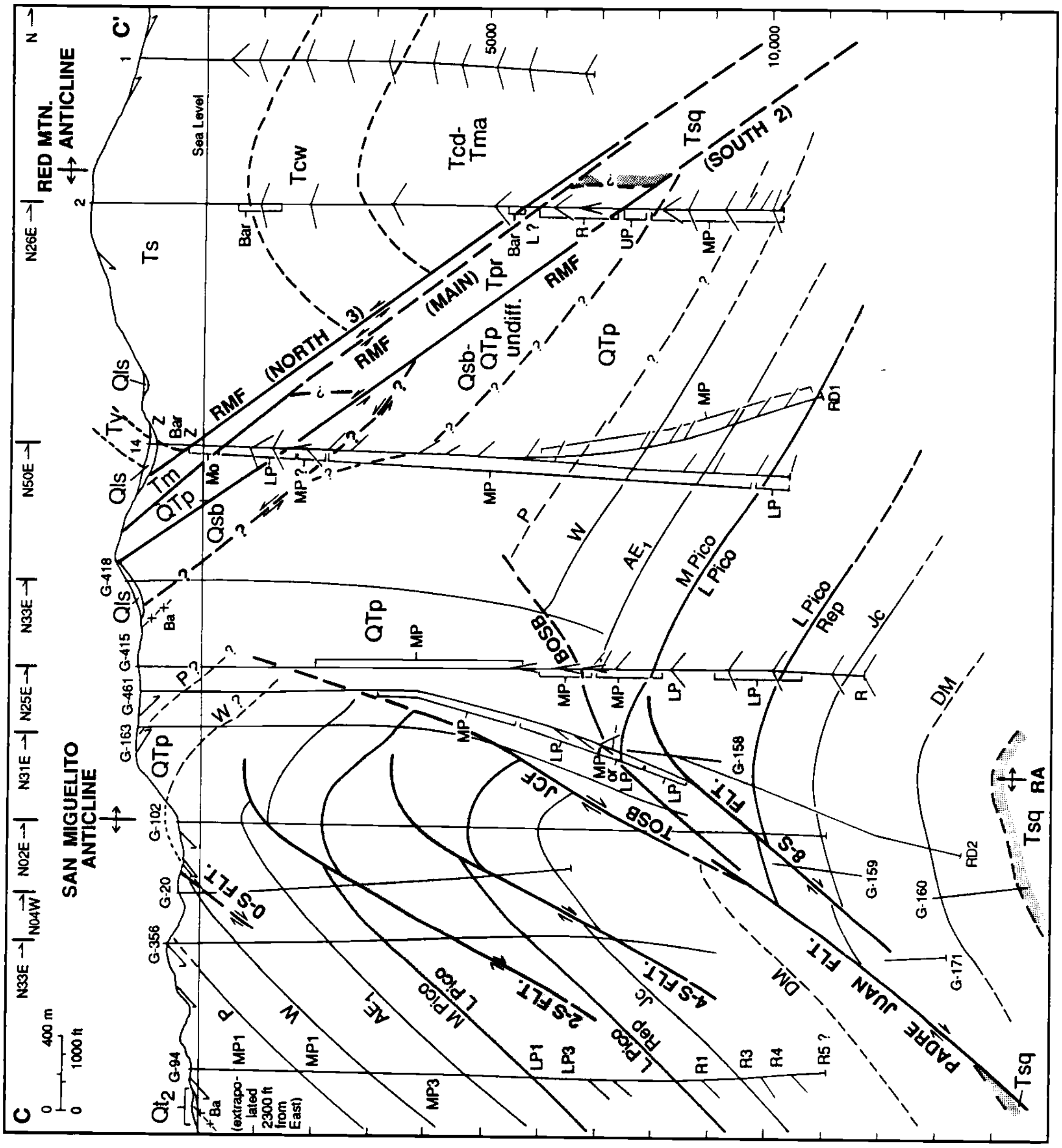
C
C'
SAN MIGUELITO ANTICLINE
RED MTN. ANTICLINE
400 m
1000 ft
(extrapo-lated 2300 ft from East)
Sea Level
5000
10,000
N33E
N04W
N02E
N31E
N25E
N33E
N50E
N26E
N
RMF (NORTH 3)
RMF (MAIN)
RMF
(SOUTH 2)
TOSB
BOSB
JCF
PADRE JUAN FLT.
0-S FLT.
2-S FLT.
4-S FLT.
8-S FLT.
Ts
Tcw
Tcd-Tma
Tsq
Tpr
QTp
Qsb
Qsb-QTp undiff.
Qls
Tm
Ty'
Qt2
DM
Tsq RA

Figure 5B.

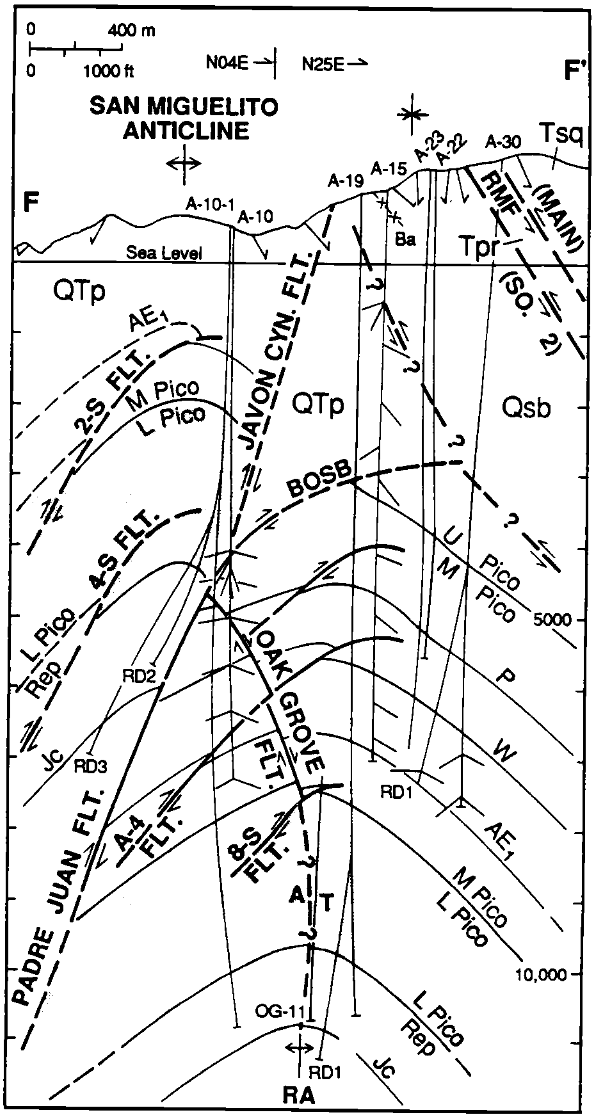
0 400 m
0 1000 ft
N04E
N25E
F'
SAN MIGUELITO ANTICLINE
F
A-10-1
A-10
A-19
A-15
A-23
A-22
A-30
Tsq
RMF
(MAIN)
Ba
Tpr
Sea Level
(SO. 2)
QTp
AE1
2-S FLT.
JAVON CYN. FLT.
M Pico
L Pico
QTp
Qsb
BOSB
4-S FLT.
U Pico
M Pico
5000
L Pico
Rep
OAK GROVE FLT.
RD2
P
W
Jc
RD3
RD1
AE1
A-4 FLT.
8-S FLT.
PADRE JUAN FLT.
A
T
M Pico
L Pico
10,000
L Pico
Rep
OG-11
RD1
Jc
RA

Figure 5C.

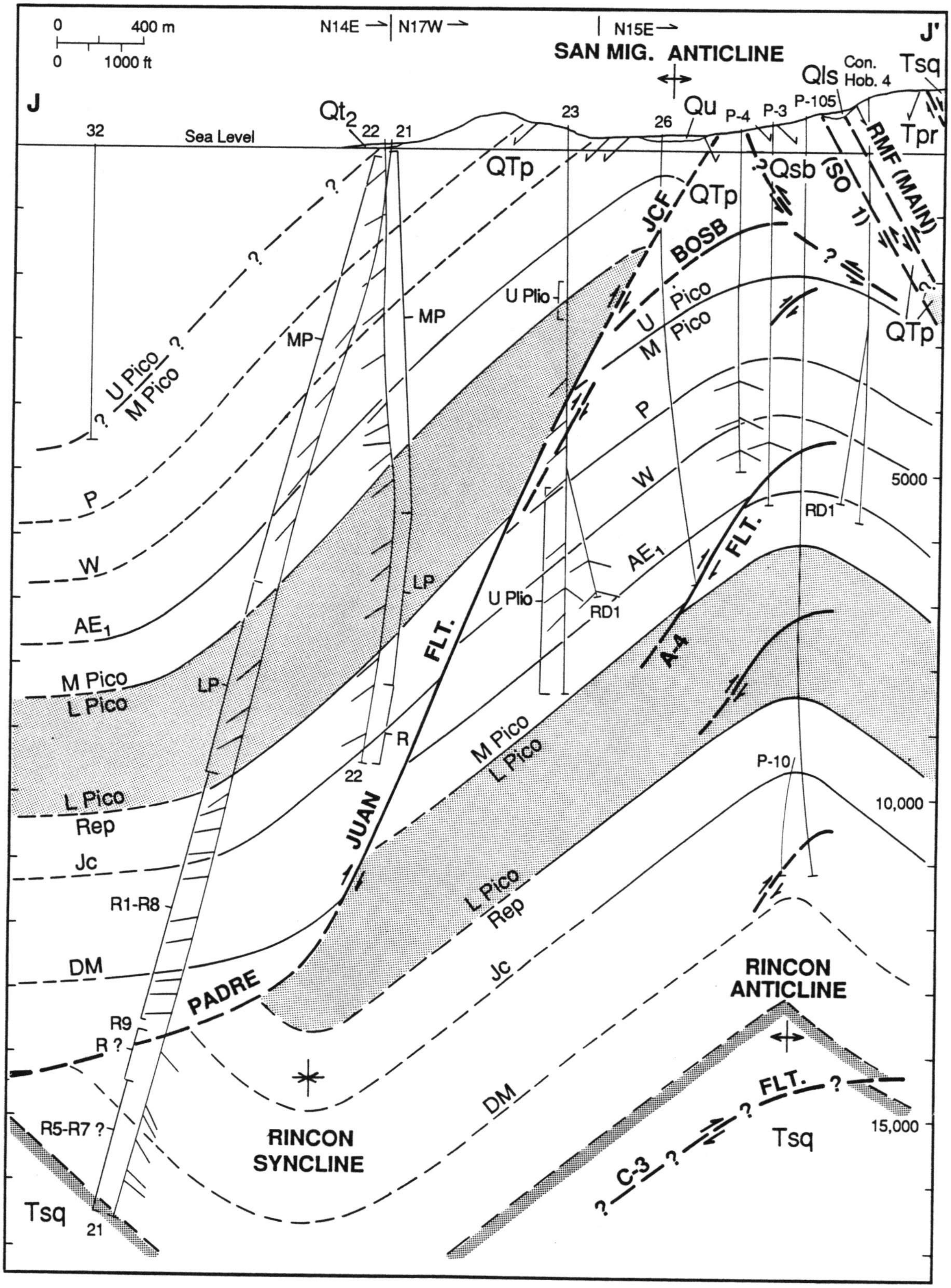
J
J'
0
400 m
0
1000 ft
N14E
N17W
N15E
SAN MIG. ANTICLINE
Sea Level
RINCON SYNCLINE
RINCON ANTICLINE
JUAN FLT.
PADRE
JCF
BOSB
RMF (MAIN)
(SO 1)
A-4
FLT.
C-3
5000
10,000
15,000
Tsq
Tpr
QTp
Qsb
Qls
Qu
Con. Hob. 4
U Pico
M Pico
L Pico
Rep
Jc
DM
P
W
AE1
U Plio
RD1
MP
LP
R
R1-R8
R9
R5-R7
P-4
P-3
P-105
P-10
32
22
21
23
26

Figure 5D.

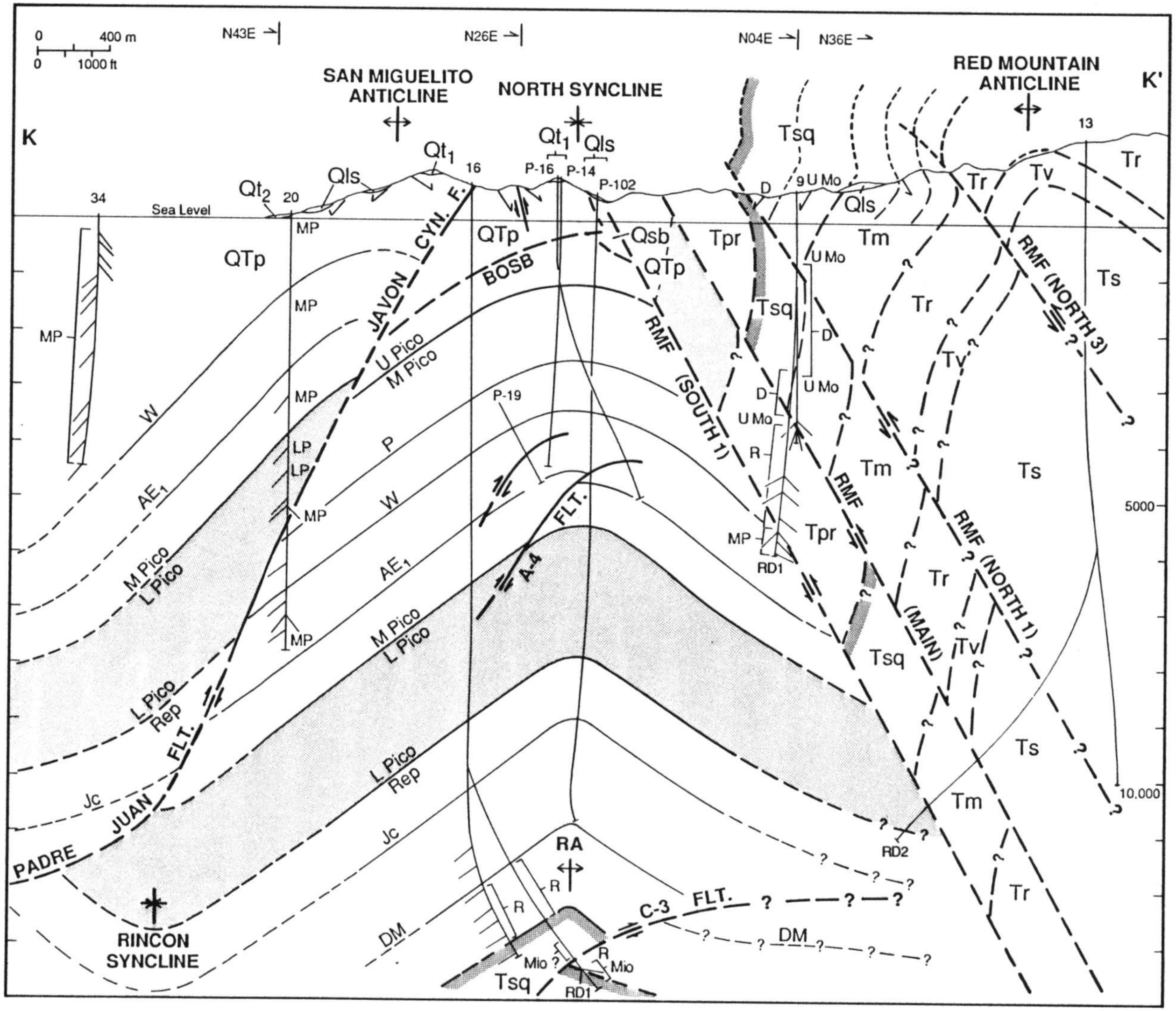

0 400 m
0 1000 ft
N43E
N26E
N04E
N36E
K
K'
SAN MIGUELITO ANTICLINE
NORTH SYNCLINE
RED MOUNTAIN ANTICLINE
RINCON SYNCLINE
RA
Sea Level
QTp
Qt1
Qt2
Qls
Qsb
Tsq
Tpr
Tm
Tr
Tv
Ts
JAVON CYN. F.
PADRE JUAN FLT.
BOSB
RMF (SOUTH 1)
RMF (MAIN)
RMF (NORTH 1)
RMF (NORTH 3)
A-4 FLT.
C-3 FLT.
U Pico
M Pico
L Pico
Rep
Jc
DM
W
P
AE1
MP
LP
U Mo
D
R
Mio
RD1
RD2
P-16
P-14
P-102
P-19
34
20
16
9
13
5000
10,000

Figure 5E.

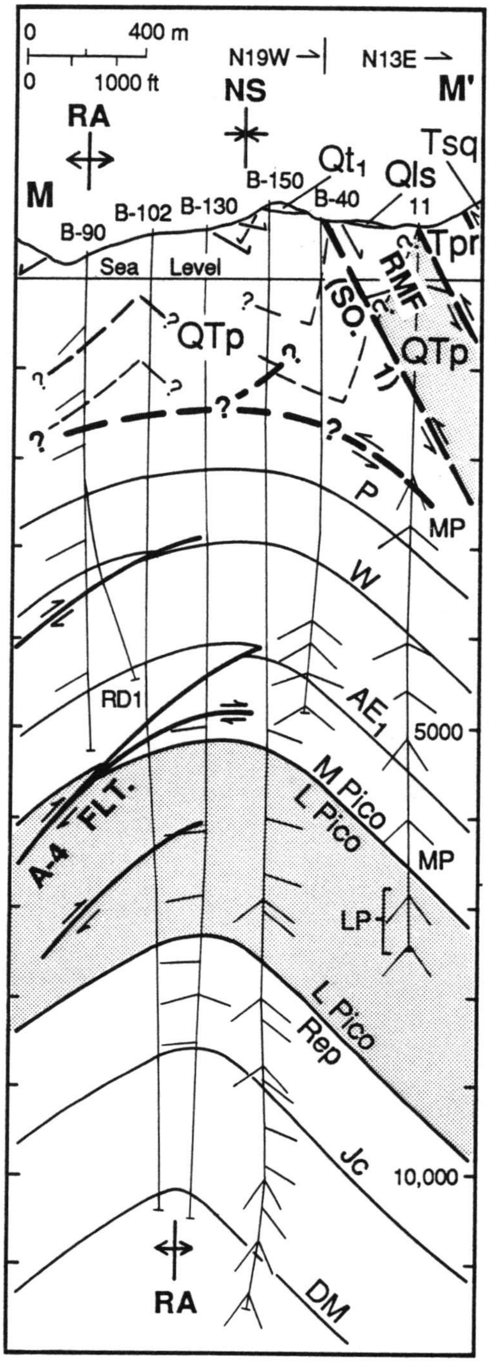

0 400 m
0 1000 ft
N19W
N13E
NS
M'
RA
M
Tsq
Qt1
Qls
B-150
B-40
11
B-90
B-102
B-130
Tpr
Sea Level
RMF
(SO. 1)
QTp
QTp
P
MP
W
RD1
AE1
5000
M Pico
L Pico
A-4 FLT.
MP
LP
L Pico
Rep
Jc
10,000
DM
RA

Figure 5F.

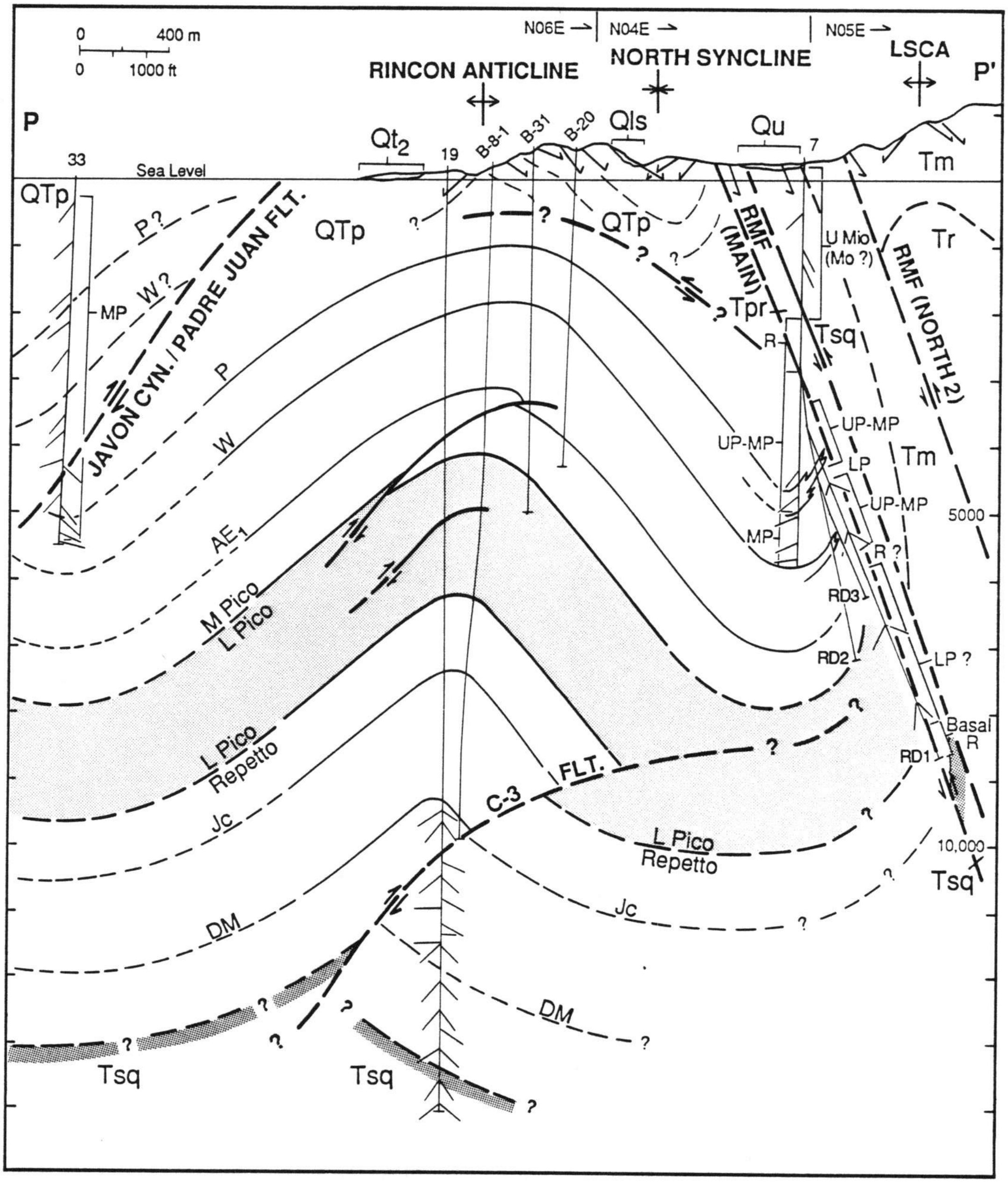

0 400 m
0 1000 ft
N06E →
N04E →
N05E →
RINCON ANTICLINE
NORTH SYNCLINE
LSCA
P
P'
Sea Level
33
19
B-8-1
B-31
B-20
7
Qt_2
Qls
Qu
Tm
QTp
Tr
U Mio (Mo ?)
RMF (MAIN)
RMF (NORTH 2)
JAVON CYN. / PADRE JUAN FLT.
Tpr
Tsq
MP
UP-MP
LP
R ?
RD3
RD2
RD1
LP ?
Basal R
5000
10,000
P
W
AE_1
M Pico
L Pico
L Pico
Repetto
Jc
DM
C-3 FLT.
Tsq

Figure 5G.

the predominantly fine-grained Rincon, Monterey, and Sisquoc Formations of Miocene to early Pliocene age (Fig. 4). These units are mechanically relatively incompetent and have deformed ductilely in and adjacent to the northern Ventura basin. They are tectonically thickened and thinned north of the Red Mountain fault and are highly attenuated where juxtaposed against it. At Carpinteria the thickness of the Rincon and Monterey Formations totals 1250 m (4100 ft) (Jackson and Yeats, 1982). On the south limb of the Red Mountain anticline against the Red Mountain fault, these units are approximately 900 m (3000 ft) thick (Fig. 5E). In the same area the Sisquoc Formation is about 550 m (1800 ft) thick. Other than in the hanging wall block of the Red Mountain fault, the Sisquoc Formation is the oldest formation penetrated by wells in the study area.

Plio-Pleistocene Geology

The Red Mountain fault cuts into the Ventura basin where it goes offshore west of the study area (Fig. 1). Onshore, only a small amount of Pliocene strata younger than the Sisquoc Formation is entrained in the Red Mountain fault zone and none is found north of it.

South of the Red Mountain fault, the axial trough of the Ventura basin was at lower bathyal to abyssal depths from the late Miocene into the early Pliocene (Natland, 1952, 1957; Ingle, 1980). The Sisquoc Formation was deposited during this time of maximum water depth in the basin and of initial uplift in the regions adjacent to it. The uplift caused the cessation of the fine-grained biogenic deposition that had persisted since the early Miocene and resulted in the onset of rapid clastic sedimentation. The Sisquoc grades upward to the thick turbidite deposits characteristic of Ventura basin Plio-Pleistocene deposition.

Yeats (1978) documented subsidence rates in the Ventura area which accelerated from less than 0.25 mm/yr (0.01 in/yr) in the Miocene to greater than 1.5 mm/yr (0.06 in/yr) in the early Pliocene. Ingle (1980) estimated that sedimentation rates for turbidites laid down from the Repettian through Wheelerian microfaunal Stages (Natland, 1952) were on the order of 2.0 mm/yr (0.08 in/yr). Hence, in the Pliocene and early Pleistocene, the basin shallowed. The turbiditic strata are here called the Repetto Formation (Repettian Stage) and Pico Formation (Venturian and early Wheelerian Stage) in accordance with oil industry usage. Pico and Repetto strata were deposited in less than 3 Ma (cf. Plate 2 in Yeats, 1979), yet are greater than 4,000 m (13,000 ft) thick in the center of the basin and about 3350 m (11,000 ft) thick to the west at Rincon oil field (Paschall, 1954). Thickness and sand percentage trends indicate deposition was into an elongate west-trending trough that had its distal end to the west (Hsü, 1977; Hsü et al, 1980). Immediately south of the Red Mountain fault, Pico and Repetto strata are finer grained than time-equivalent rocks found in the San Miguelito and Rincon oil fields farther south. A similar sandstone to mudstone facies change occurs east of the Red Mountain fault in the time-equivalent section that crops out in the north flank of the Cañada Larga syncline. This facies change extends southwest, parallel to the east end of the Red Mountain fault (Yeats et al, in press), towards the study area. Red Mountain and the nearby area apparently acted as a submarine high, perhaps a sea knoll, during much of the Pliocene (Yeats et al, in press).

In the early Pleistocene, the conditions of ubiquitous subsidence within the basin changed to more varied, localized subsidence. At Ventura, Yeats (1983) documented intraformational north-dipping blind thrust faulting in the Repetto and Pico Formations. The age of faulting is constrained to 1.3 to 0.65 Ma ago based on local thinning and fining of units above the faults. In the study area, an abrupt transition upwards from turbiditic to monotonously fine-grained strata occurs across the north half of Rincon oil field. Exposures of 1.2 Ma old Bailey ash (Izett et al, 1974) occur near the base of the fine-grained unit (Sarna-Wojcicki et al, 1979, 1984; Liddicoat and Opdyke, 1981). The mudstone above the facies change horizon is the time and lithologic equivalent of the shallow marine "Mud Pit shale" member of the Santa Barbara Formation found at Ventura. The "Mud Pit shale" is considered to be the "upper" member of the Pico Formation by Hacker (1970), but its megafauna can be correlated with that of the type Santa Barbara Formation (Woodring et al, 1940); hence, the name "Santa Barbara Formation" is used here. At Ventura Avenue oil field the "Mud Pit shale" is conformable above Pico turbidites and is 280 to 530 m (900 to 1700 ft) thick on the flanks of the Ventura Avenue anticline. At Carpinteria, north of the Red Mountain fault, the Santa Barbara Formation consists of fine- to medium-grained sandstone, siltstone, and interbedded claystone and conglomerate lenses. It is unconformable over predominantly Miocene and older strata, and it is up to 1080 m (3540 ft) thick (Jackson and Yeats, 1982). True thickness of the Santa Barbara Formation in the study area is unknown because the upper surface is everywhere eroded or juxtaposed against the Red Mountain fault. Minimum thickness is approximately 550 m (1800 ft).

In the study area, all subsurface contacts above the Sisquoc Formation are based on the benthic foraminifera biostratigraphy of Natland (1952) and on recognized electric-log markers. Because index species occurrences most commonly used in defining biostratigraphic units are related to water depth, they are not synchronous across the Ventura and Los Angeles basins (cf. Natland, 1952; Bandy, 1960; Ingle, 1967). Where possible, contacts used in this paper (Fig. 3) are based on electric log divisions employed by the oil companies operating in the area, and are only loosely tied to Natland's biostratigraphy.

In the Ventura area and farther east, subsidence accelerated following deposition of the "Mud Pit shale". Rates of deposition of up to 2.0 mm/yr (0.08 in/yr) (Yeats, 1978) characterize the Saugus (San Pedro) Formation (Putnam, 1942). Saugus deposition began 600,000 years ago, ended less than 200,000 years ago in the Ventura area (Lajoie et al, 1982), and in that time accumulated to 1000 m (3300 ft) thickness. The youngest Saugus preserved today in the Ventura area is at the unconformity surface beneath the Ventura Marine terrace where the age of *Protothaca* mollusc shells was estimated to be approximately 205,000 years by amino-acid racemization methods (Wehmiller et al, 1978). The onset of the present episode of uplift in the western Ventura basin may be coincident with the cessation of Saugus deposition at about this time. In the study area no Saugus is preserved.

Surficial Deposits and Landslides

Three sets of dated marine terrace benches are cut into the folded Plio-Pleistocene strata in the Ventura area. The oldest is the 85,000 to 105,000 year old Ventura Marine terrace, found on the south flank of the Ventura Avenue anticline east of the Ventura River (Lajoie et al, 1979, 1982). At Ventura these deposits dip 9° to 15° south and stand 30 to 175 m (95 to 575 ft) above sea level. The nearly flat-lying Punta Gorda Marine terrace, dated at 40,000 to 60,000 years old by amino-acid racemization (Wehmiller et al, 1978; Lajoie et al, 1982) and by U-series methods (Kaufman et al, 1971), can be traced from near sea level 8 km (5 mi) northwest of the study area to 255 m (835 ft) above sea level near Pitas Point, above the crest of the Rincon anticline (Fig. 3). The Sea Cliff Marine terrace (Putnam, 1942) stretches in a narrow band just landward of the present coastline from the Ventura River to Punta Gorda (Fig. 3). Over the crest of the Rincon anticline between Pitas Point and Punta Gorda, the terrace attains a maximum elevation of 37 m (120 ft). Radiocarbon dating of mollusc shells from the terrrace yields ages between 1800 and 5800 years old (Lajoie et al, 1979; 1982).

North of Ventura, the Ventura River eroded through the Ventura Avenue anticline and the hanging wall block of the Red Mountain fault and left a number of stranded fluvial terrace benches on the older strata. Radiocarbon dating of deposits on these terrace benches and correlation with the Ventura basin soils chronosequence suggest ages ranging from historical to 80,000 years in age (Keller et al, 1982; Rockwell et al, 1984).

The effect of rapid folding and uplifting of northern Ventura basin strata and of differential erosion of those strata has been to form an area of high relief and steep slopes adjacent to the shoreline west of Ventura. The Pliocene and Pleistocene strata that crop out in this area are poorly consolidated, resulting in unstable slopes and many landslides. The geologic map (Fig. 3) shows landslides to be especially concentrated along the surface traces of faults.

QUATERNARY STRUCTURES

The structures in and bounding the northern Ventura basin reflect the compressive tectonism that has marked basin deformation in the Quaternary. Especially prominent are the basinal late Pleistocene to Holocene folds and faults of the Ventura Avenue-Rincon anticlinal trend. In the study area, two other sets of structures are also found. They are 1) basinal early Pleistocene structures and 2) the Red Mountain fault system and associated hanging wall folds.

Red Mountain Fault System

The Red Mountain fault system is the set of closely spaced, north-dipping reverse faults that form the northern boundary of the Ventura basin in the study area. Six strands of the fault are recognized (Fig. 3). The Main Strand of the Red Mountain fault has been contoured from its eastern terminus north of Ventura to its western terminus in the Santa Barbara Channel (Jackson, 1981; Jackson and Yeats, 1982; Yeats et al, in press). A fault contour map for the Main Strand of the fault in the study area, slightly modified from Jackson and Yeats (1982) and Yeats et al (in press), is shown in Figure 6.

Maps and cross-sections showing the Main Strand of the Red Mountain fault imply that it is always separable from the other strands mapped in the study area. The

Figure 6: Fault contour map. Contours on Javon Canyon/Padre Juan, C-3, and main branch of Red Mountain faults. Contours relative to sea level; in feet. Shaded region represents the Javon Canyon fault surface where it is above the Padre Juan fault surface.

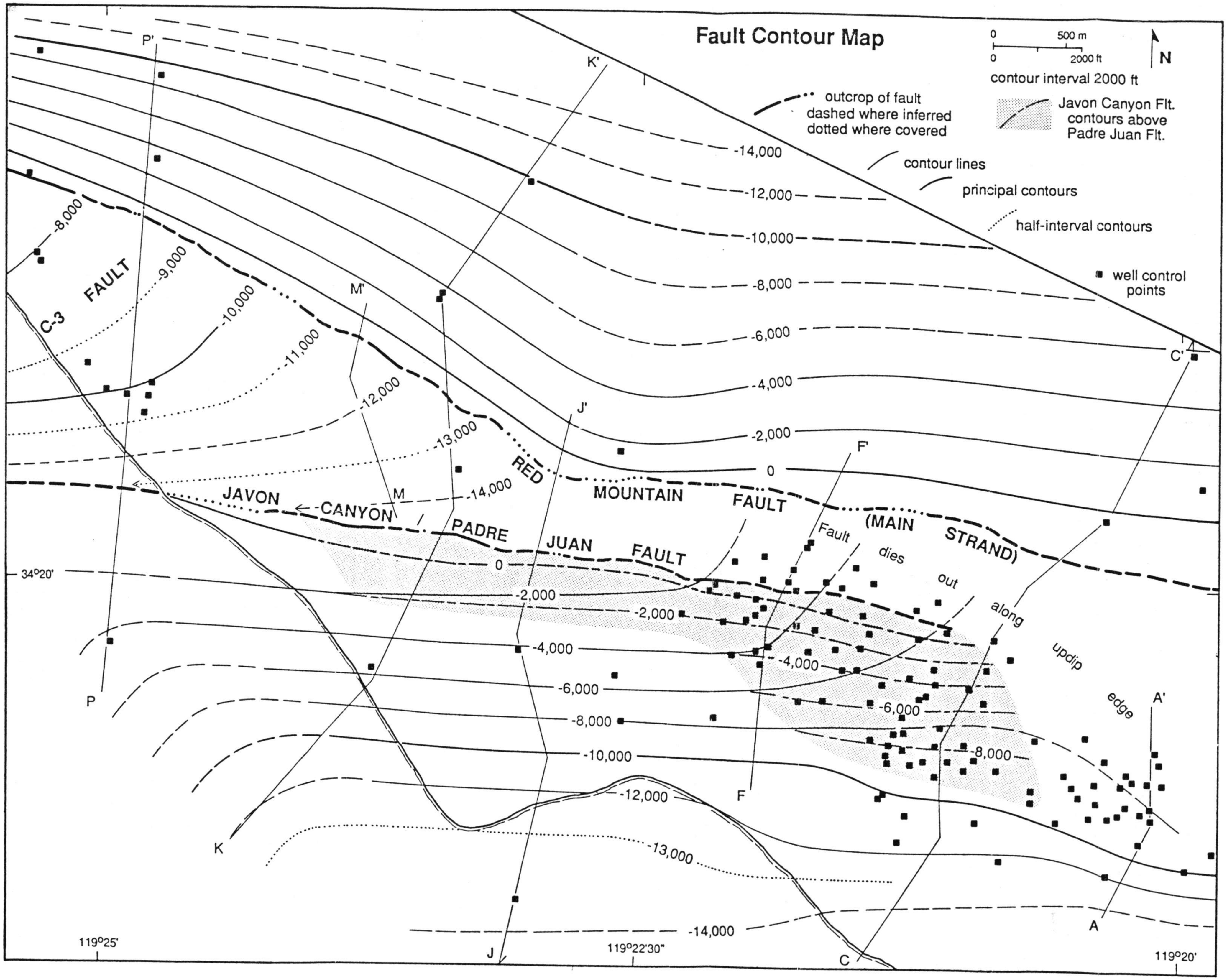
Fault Contour Map
0 500 m
0 2000 ft
N
contour interval 2000 ft
outcrop of fault
dashed where inferred
dotted where covered
Javon Canyon Flt.
contours above
Padre Juan Flt.
contour lines
principal contours
half-interval contours
well control points
C-3 FAULT
RED MOUNTAIN FAULT (MAIN STRAND)
JAVON CANYON
PADRE JUAN FAULT
Fault dies out along updip edge
-14,000
-12,000
-10,000
-8,000
-6,000
-4,000
-2,000
0
-9,000
-11,000
-13,000
34°20'
119°25'
119°22'30"
119°20'

Figure 6.

difficulty in identifying fault traces in the field and the small amount of subsurface control on individual fault strands suggests that the nature of the fault system may be more complex than shown. It can be seen, however, that 1) South Strand 1 of the Red Mountain fault, which offsets Punta Gorda terrace deposits, is distinguishable from the Main Strand of the fault in the subsurface by repeated microfossil zones in well 9 (Fig. 5E), 2) North Strand 2 is the same as the North Branch of the Red Mountain fault of Jackson and Yeats (1982), and 3) North Strand 3, which is inferred in surface maps to diverge northwestward away from the Main Strand of the Red Mountain fault, and to parallel the northwest plunging nose of the Red Mountain anticline, exists above the Main Strand of the fault in well 2 (Fig. 5B).

From its eastern terminus, the Main Strand of the Red Mountain fault strikes south and then southwest around the eastern nose of the Red Mountain anticline (Fig. 1). West of Ventura, reverse separation increases and the fault curves west around the south side of Red Mountain. It trends N60W where the Red Mountain anticline plunges west beneath Miocene strata, and N80W where it goes offshore. West from Javon Canyon, the dip of the fault steepens from near 60° to more than 80° north (Fig. 6; compare Figs. 5B, 5E, and 5G). Rather than becoming conformable with bedding at depth, as is the case with the south-dipping faults, the Red Mountain fault continues to cut downdip into pre-Tertiary competent strata (Yeats et al, in press).

Across the fault zone on the surface, footwall strata of the Pico and Santa Barbara Formations are juxtaposed against highly deformed strata of the Pico, Repetto, and Sisquoc Formations. Pico and Repetto rocks do not occur north of the Red Mountain fault zone in the study area. In the subsurface, strata as old as the Eocene Matilija Sandstone are penetrated in the hanging wall block of the fault. In the footwall, Wheelerian Stage "upper" Pico (Santa Barbara ?) beds are truncated at greater than 3050 m (10,000 ft) depth (Fig. 5B).

Displacement across the Red Mountain fault zone can most accurately be measured in the Padre Juan Canyon area where the base Repetto-top Sisquoc contact can be extrapolated to the faulted zone in both the hanging wall and footwall blocks (Figs 5E, 7A). Reverse separation (i.e. dip-slip displacement measured in the plane of the fault) across the faulted zone at balanced cross-section J-K' (Fig. 7A) is approximately 5850 m (19,200 ft). Displacement is greatest in the Cañada del Diablo area, where reverse separation of the Repetto-Sisquoc contact is a maximum of 7300 m (23,950 ft) (Fig. 5B). Here Yeats et al (in press) estimated a minimum of 5500 m (18,000 ft) of stratigraphic separation (i.e. vertical

Figure 7: Balanced cross-section J-K'. A) Present. Location of cross-section line shown in Figure 2. See Figure 3 for legend. Cross-section balanced between trace of Pitas Point fault or flexure and Red Mountain fault. Pitas Point fault not documented in this study; its position is based on a steep flexure in seismic lines (Greene et al, 1978; Yeats, 1981). Geology shown in hanging wall of Red Mountain fault used to estimate displacement across the fault zone. B) Cross-section J-K' restored for region south of Red Mountain fault. See text for explanation of points X and Y.

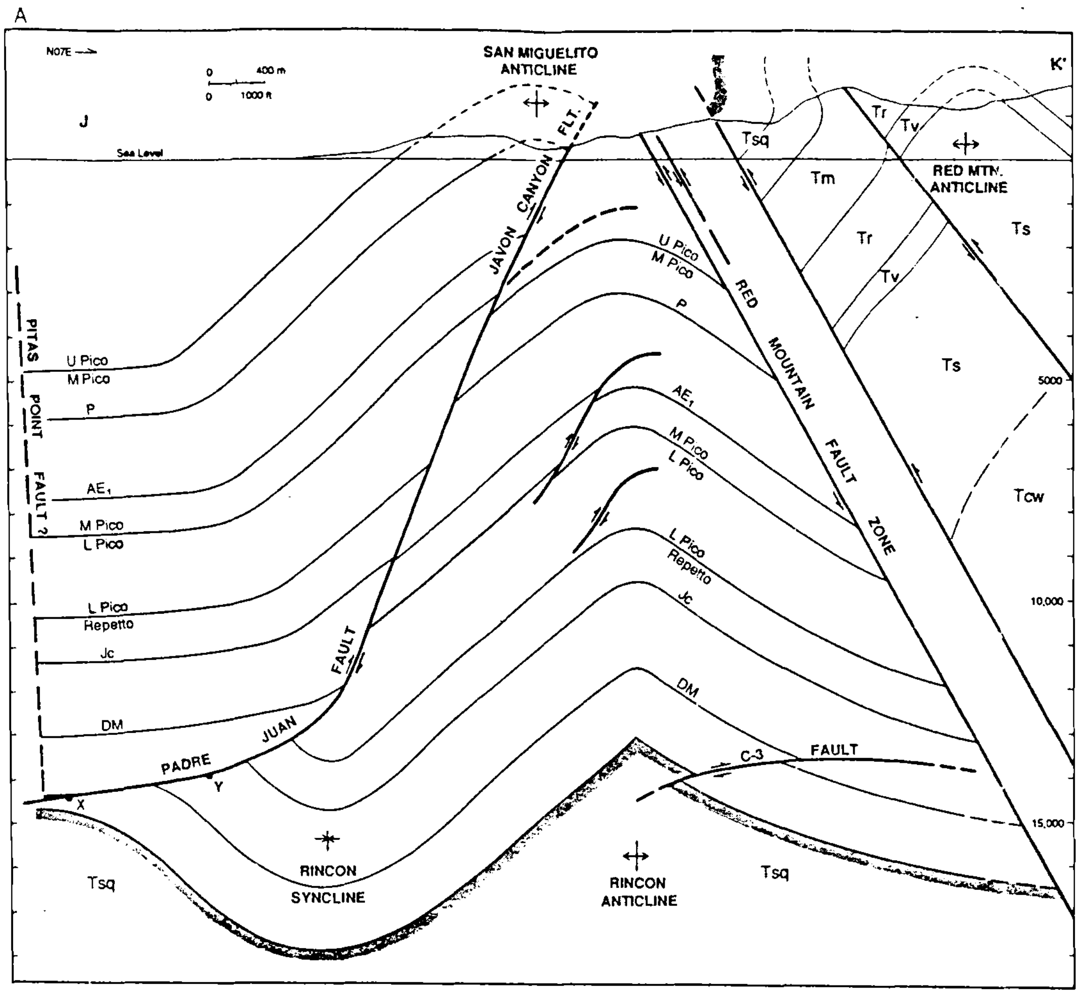
A
N07E
0 400 m
0 1000 ft
SAN MIGUELITO
ANTICLINE
J
Sea Level
K'
Tsq
Tr
Tv
RED MTN.
ANTICLINE
Tm
Ts
Tr
Tv
Ts
Tcw
5000
10,000
15,000
JAVON CANYON FLT.
U Pico
M Pico
P
AE1
M Pico
L Pico
L Pico
Repetto
Jc
DM
RED MOUNTAIN FAULT ZONE
PITAS POINT FAULT ?
U Pico
M Pico
P
AE1
M Pico
L Pico
L Pico
Repetto
Jc
DM
FAULT
PADRE JUAN
C-3 FAULT
X
Y
Tsq
RINCON
SYNCLINE
RINCON
ANTICLINE
Tsq

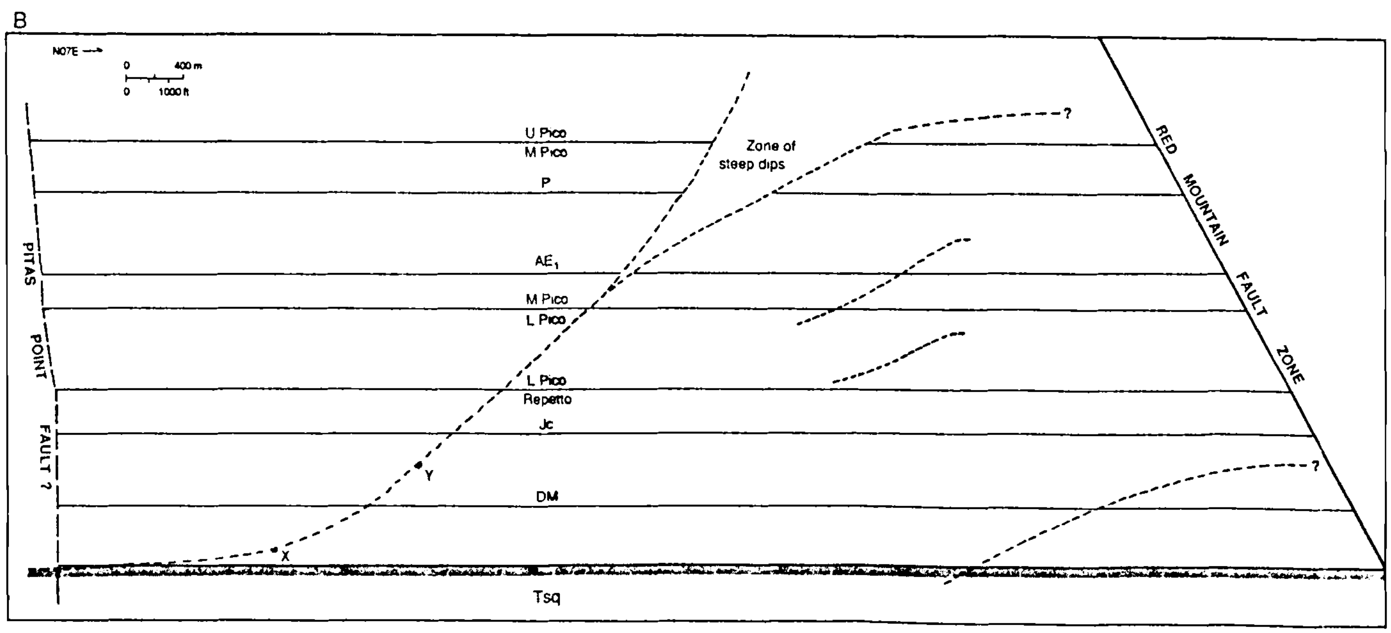
B
N07E
0 400 m
0 1000 ft
U Pico
M Pico
Zone of
steep dips
P
AE1
M Pico
L Pico
L Pico
Repetto
Jc
DM
?
?
Y
X
RED MOUNTAIN FAULT ZONE
PITAS POINT FAULT ?
Tsq

Figure 7.

displacement of an offset horizon) at the top Oligocene sandstone (Vaqueros Formation) horizon. At cross-section J-K' there is a maximum of 6750 m (22,150 ft) of stratigraphic separation. As much as 1900 m (6200 ft) of this value results from the development of the Red Mountain anticline. At cross-section P-P' (Fig. 5G), reverse separation reduces to no more than 4800 m (15,750 ft) and stratigraphic separation of the top Monterey Formation to less than 5300 m (17,400 ft). 6.5 km (4.0 mi) farther west, reverse separation of the top Sisquoc Formation is only 365 m (1200 ft) (Jackson and Yeats, 1982).

The Red Mountain fault system is still active. West of Los Sauces Canyon the Main Strand offsets 45,000 year old Punta Gorda terrace deposits 22 m (72 ft) vertically, resulting in a separation rate of 0.5 to 0.6 mm/yr (0.019 to 0.023 in/yr) (Geotechnical Consultants, 1968; Jackson and Yeats, 1982). Offsets of the Punta Gorda terrace between Javon and Madranio Canyons yield comparable displacement rates of 0.5 to 1.6 mm/yr (0.019 to 0.06 in/yr) (Sarna-Wojcicki et al, 1979). Additionally, Yeats et al (in press) attribute a 1970-75 series of earthquakes (M>1) to the Red Mountain fault system. Epicenters were concentrated at approximately 5 to 12 km (3.1 to 7.5 mi) depth in a region centered approximately

5 km (3.1 mi) north of the surface expression of the fault zone in the study area. They were linked to the surface trace of the Main Strand of the fault along an approximately 60° north-dipping fault plane.

The doubly-plunging Red Mountain anticline is located approximately 2.5 km (1.5 mi) north of the region of maximum separation of the Red Mountain fault system. To the east, it disappears beneath Quaternary alluvium of the Ventura River bed. To the west, it dies out in Rincon and Monterey Formation strata just beyond Javon Canyon. Evidence indicates folding is related to Red Mountain faulting: 1) The fold dies out to both the east and west as fault separation decreases; 2) North Strand 3 of the Red Mountain fault, which diverges away from the main fault system in a westerly direction, appears to have formed synchronously with the anticline in its failed south limb; and 3) the Red Mountain anticline is south of older west-trending structures (structures north of the dotted line in Figure 1) that are continuous between Ojai and Carpinteria. The older structures dip south into the Ventura basin and are steeply unconformable beneath the Santa Barbara Formation in the Carpinteria area and beneath the Saugus Formation in the Ojai area. They probably predate major Plio-Pleistocene reverse motion on the Red Mountain fault (Jackson and Yeats, 1982). The Ayers Creek syncline, located just north of the Red Mountain anticline (Fig. 1), is also south of these older structures, and probably formed synchronously with the Red Mountain anticline.

The Los Sauces Creek anticline in the hanging wall of North Branch 2 of the Red Mountain fault, also lies south of the older structures referred to above. It folds Miocene rocks that are unconformable beneath Santa Barbara and younger strata, suggesting possible activity on North Branch 2 prior to Santa Barbara Formation deposition.

Early Pleistocene Ventura Basin Structures

Evidence for early Pleistocene compressive deformation south of the Red Mountain fault system is found east of the study area near Ventura. Yeats (1979; 1983) documented the initiation about 1.3 Ma ago of reverse motion on a series of north-dipping blind thrust faults (Taylor fault set) which originated in silty, fine-grained horizons of the Repetto Formation and caused upwarping in the sea floor above them. Because of the localized positive relief, sediment thicknesses are greater and facies coarser on the downthrown side of the faults in strata older than 0.65 Ma (see Fig. 5a in Yeats, 1983). Younger strata do not show stratigraphic variation across the faults, indicating fault activity ceased after 0.65 Ma ago. All faults of the Taylor set are folded over the Ventura Avenue anticlinal axis and continue upsection as low angle structures in the south limb of the fold (cf. Figs. 7, 8 in Yeats, 1982). Pre-fold restoration of Taylor fault planes shows they formerly had east-northeast strikes approximately parallel to the east end of the Red Mountain fault, inferring uplift or reduced subsidence in the area of the Red Mountain seaknoll between 1.3 and 0.65 Ma ago. With one possible exception (Fig. 5A), no Taylor faults are identified west of Ventura Avenue oil field.

In the north half of Rincon oil field, the upward transition from the silty-sandy Pico Formation to the monotonously fine-grained deposits of the Santa Barbara Formation may be an unconformity surface. Electric log correlations indicate progressively lower stratigraphic horizons in the Pico are truncated in a north direction (Figs. 5C, 5D), suggesting possible uplift or reduced subsidence of the northern edge of the basin towards the Red Mountain seaknoll. The occurrence of Bailey ash near the base of the fine-grained unit at Hill 1192 (Figs. 2, 3) and just beneath it near cross-section C-C' (Fig. 5B), constrains the time of change to about 1.2 Ma ago or slightly earlier. The facies change horizon also may have served later as a surface of detachment beneath the toe of the Red Mountain fault; possibly it is an extension of the shallow detachment seen farther west (discussed below).

Two other early Pleistocene structures occur in the Ventura basin in the study area. These are the Oak Grove and Grubb faults, both of which strike northwest in contrast to the generally west-trending late Pleistocene structures in the basin. The Oak Grove fault (Figs. 5C, 8) is mapped in the subsurface in the Padre Juan Canyon area and is recognized only beneath the Padre Juan fault. The fault strikes N25W to N35W, dips steeply northeast, and has a maximum apparent normal separation of 105 m (350 ft) where mapped, though values from well to well are highly variable. It is not known how far north the Oak Grove fault extends towards the Red Mountain fault. The inability to find the Oak Grove fault in wells below -2000 m (-6550 ft) suggests either that the fault dies out downsection or that dips steepen from about 65° to become vertical or overfolded. To the southeast, just beyond the A-10 and A-10-1 wells (Fig. 5C), the fault is truncated by the overlying Padre Juan fault. It may be cut by the A-4 and other south-dipping faults. Late Pleistocene differential folding apparently occurred across a preexisting Oak Grove fault surface because there is 120 to 150 m (400 to 500 ft) of apparent right-lateral separation of the Rincon anticlinal axis at the "AE_1" horizon (Fig. 8).

The Grubb fault (Figs. 5A, 9A), which separates the

Figure 8: Map view of surface and "shallow" subsurface structural elements. "P" and "AE_1" are electric log horizons in the "middle" Pico Formation; "P" is approximately 550 m (1800 ft) stratigraphically above "AE_1". The south offset of the surface trace of the San Miguelito anticline from its trace at the "AE_1" horizon is due to the occurrence of intervening minor south-dipping reverse faults between the two axial traces. South offset of surface Rincon anticline axial trace from "P" horizon trace is probably the result of displacement of surface and near-surface strata southward above a shallow detachment propagated in front of South Strand 1 of the Red Mountain fault. JC/PJF, Javon Canyon/Padre Juan fault; VAA, Ventura Avenue anticline.

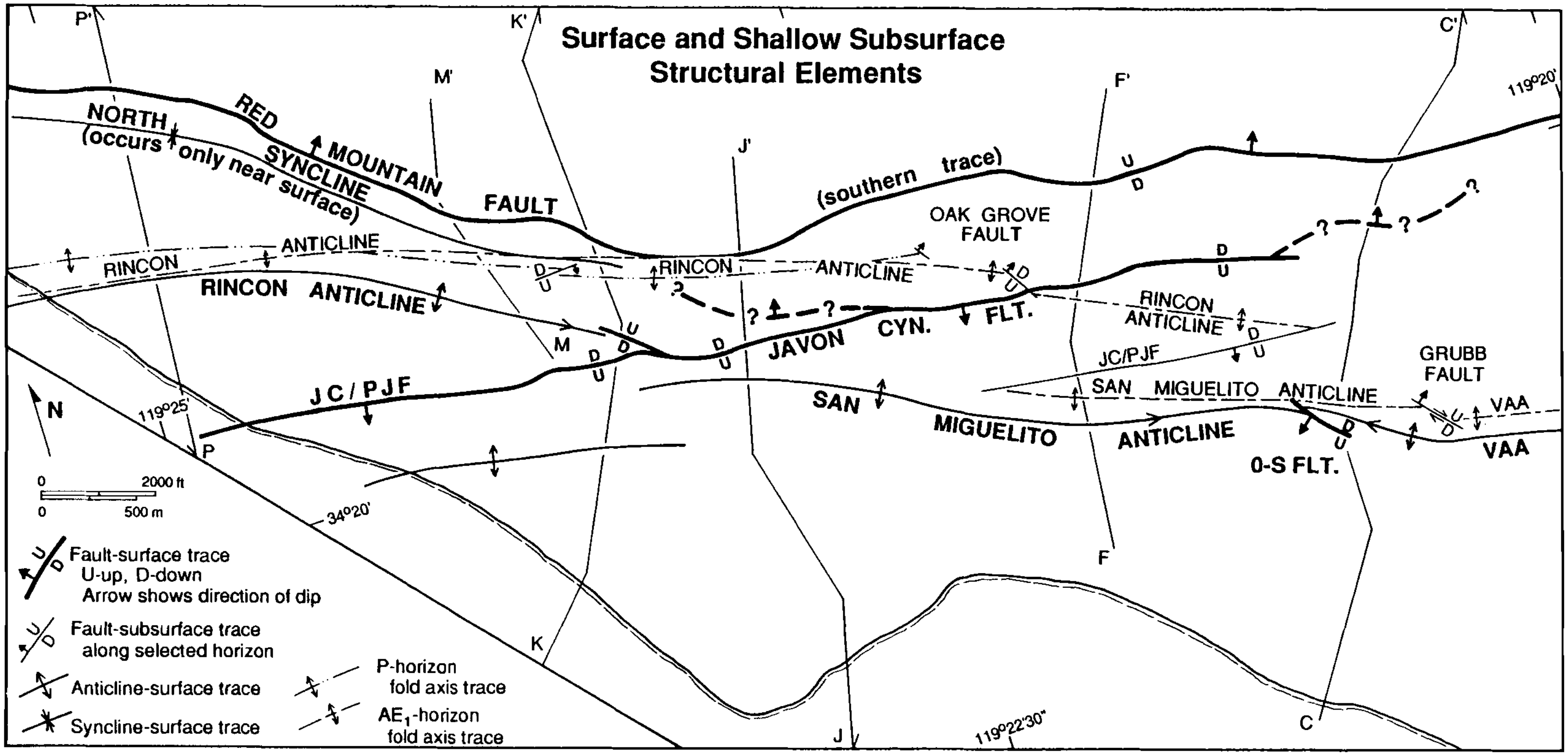
Surface and Shallow Subsurface
Structural Elements
P'
K'
M'
J'
F'
C'
119°20'
NORTH
(occurs only near surface)
SYNCLINE
RED MOUNTAIN FAULT
(southern trace)
OAK GROVE
FAULT
RINCON ANTICLINE
RINCON ANTICLINE
RINCON ANTICLINE
RINCON
ANTICLINE
JAVON CYN. FLT.
JC/PJF
JC/PJF
SAN MIGUELITO ANTICLINE
SAN MIGUELITO ANTICLINE
GRUBB
FAULT
VAA
VAA
0-S FLT.
N
119°25'
P
M
34°20'
K
J
F
C
119°22'30"
0
2000 ft
0
500 m
Fault-surface trace
U-up, D-down
Arrow shows direction of dip
Fault-subsurface trace
along selected horizon
Anticline-surface trace
Syncline-surface trace
P-horizon
fold axis trace
AE_1-horizon
fold axis trace

Figure 8.

Figure 9: A) Structure contour map of "Jc" electric log horizon (in Repetto Formation). "Jc" horizon is equivalent to "AO" horizon at Ventura Avenue oil field. Shading represents regions where the "Jc" horizon overlaps in the hanging wall and footwall blocks of reverse faults. Contours relative to sea level; in feet. GF, Grubb fault; SMA, San Miguelito anticline; VAA, Ventura Avenue anticline. B) Isoseparation map for "Jc" horizon across the Javon Canyon/Padre Juan fault. Contours given in feet; values represent vertical distance between "Jc" horizon in hanging wall of fault from "Jc" horizon in footwall.

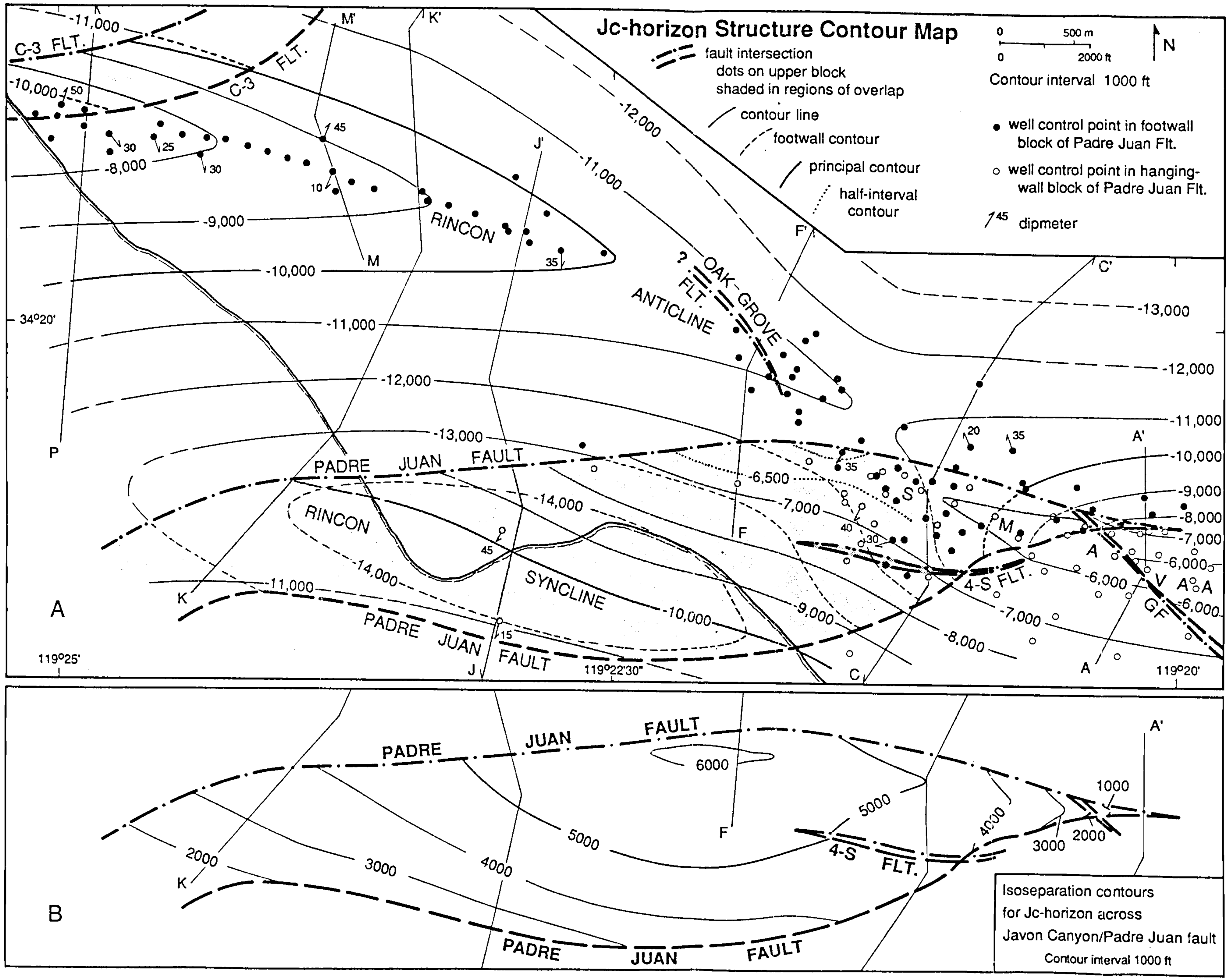
Jc-horizon Structure Contour Map
fault intersection
dots on upper block
shaded in regions of overlap
contour line
footwall contour
principal contour
half-interval contour
Contour interval 1000 ft
well control point in footwall block of Padre Juan Flt.
well control point in hanging-wall block of Padre Juan Flt.
dipmeter
0 500 m
0 2000 ft
N
C-3 FLT.
RINCON
OAK GROVE FLT.
ANTICLINE
PADRE JUAN FAULT
RINCON SYNCLINE
4-S FLT.
34°20'
119°25'
119°22'30"
119°20'
A

B
PADRE JUAN FAULT
4-S FLT.
Isoseparation contours for Jc-horizon across Javon Canyon/Padre Juan fault
Contour interval 1000 ft

Figure 9

Ventura Avenue anticline from the San Miguelito anticline, is mapped in the subsurface near the San Miguelito-Ventura Avenue oil field boundary. It is identified only above the Padre Juan fault, yet cannot be recognized at the surface. The Grubb fault can be traced to the southeast into the Ventura Avenue oil field (Hsü, 1977); to the northwest it cannot confidently be traced far beyond the axis of the San Miguelito anticline. The northeast-dipping fault surface steepens to vertical and may be overfolded, and changes from apparent reverse to apparent normal separation as it passes north of the axis of the Ventura Avenue anticline.

On the "Jc" horizon, the Ventura Avenue-San Miguelito anticlinal axes are offset approximately 180 m (600 ft) in a right-lateral sense across the Grubb fault (Fig. 9A). The north-dipping Taylor reverse fault (Hsü, 1977) is truncated abruptly to the southwest against the Grubb fault (Yeats, 1983). The Padre Juan fault cannot be traced significantly far east beyond the Grubb fault into the Ventura Avenue oil field (R. O. Beringer, pers. commun., 1984). Late Pleistocene south-dipping faults apparently offset the Grubb fault (Fig. 5A), but they do so in a complex way that may indicate concurrent motion on the Grubb fault.

Hsü (1977) and Yeats (1979; 1983) considered the Grubb and the Oak Grove to be tear faults that were active during motion on the Taylor fault set and that accommodated differential shortening along either side of them. Support for this reasoning comes from east of the study area where unfolding of the Taylor fault around the Ventura Avenue anticline results in a fault with a northwest directed displacement vector that is approximately parallel to the strike of the Grubb fault (Hsü, 1977). Because the Oak Grove is stepped west from the Grubb fault into an area where no Taylor-type faults are known to occur, evidence for it being an early Pleistocene tear fault is equivocal. Mapping of oil saturation levels across the Oak Grove fault, however, shows lower oil-water contacts on the south side of the Rincon anticline west of the fault and lower contacts on the north limb of the anticline east of the fault (G. J. Gregory and S. R. Fagan, pers. commun., 1984). This implies that the fault existed and formed a permeability barrier before the migration of oil associated with late Pleistocene folding.

Late Pleistocene Folding and Faulting

San Miguelito Anticline, Rincon Anticline, and Associated Folds. In the study area, the fold which is impressively exposed in the amphitheater at San Miguelito oil field (Fig. 10) has been known as the Ventura Avenue anticline because its surface trace is continuous with the well known structure to the east. Subsurface mapping near the

Figure 10: A) San Miguelito anticline exposure in west face of the San Miguelito amphitheater, San Miguelito oil field, western Ventura basin, Ventura County, California. The fold is in the Plio-Pleistocene Pico Formation. The fold and minor fault present in the photo are probably no more than 200,000 years old. B) Line drawing of San Miguelito anticline and 0-S fault in the face of San Miguelito amphitheater. Looking west; figure shows close up view of central region of photo. Dark shading represents approximate trace of 0-S fault. Light shading illustrates possible offset across the fault.

Figure 10A.

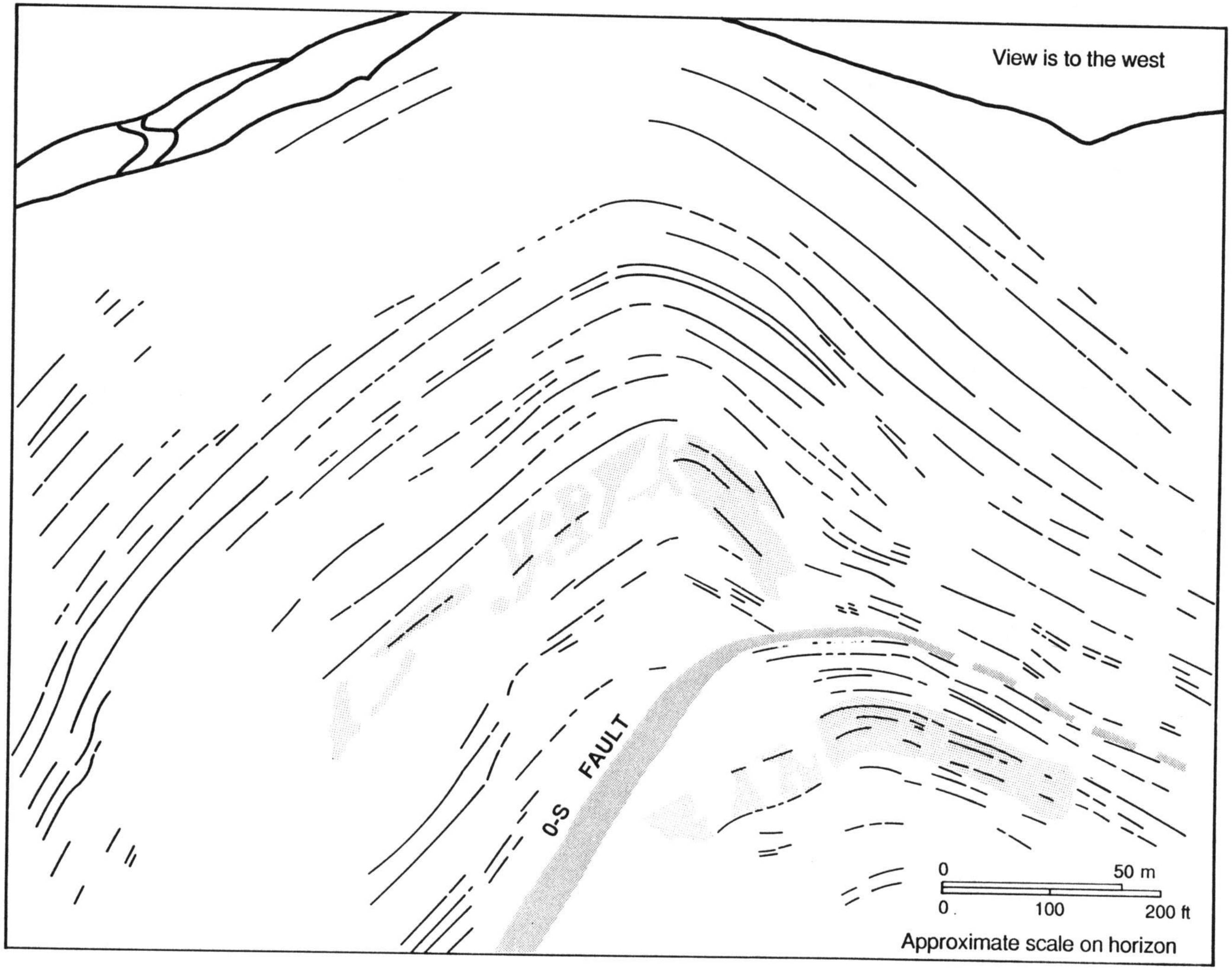
View is to the west
O-S FAULT
0
50 m
0
100
200 ft
Approximate scale on horizon

Figure 10B.

Ventura Avenue-San Miguelito oil field boundary, however, shows the Ventura Avenue anticlinal axis to be offset about 180 m (600 ft) in a right-lateral sense across the trace of the Grubb fault (Figs. 8, 9A). Here, the anticline west of the Grubb fault and above the Padre Juan fault is referred to as the San Miguelito anticline. The San Miguelito anticline differs from the Rincon anticline, which lies beneath the Padre Juan fault, because in a west direction the axial traces of the two folds diverge (compare Figures 5A-5D), rather than overlap as would be expected if they were a single fold offset by a later episode of reverse faulting.

At its eastern end, the San Miguelito anticline is markedly asymmetric. Much of the northern limb has very steep to locally overturned dips and is contained within the uncorrelatable "zone of steep beds" associated with the Padre Juan fault. South limb dips reach approximately 50° before shallowing at depth above the region of flattening of the Padre Juan fault (see well 21, Fig. 5E). At its contact with the Grubb fault, the San Miguelito anticlinal axis trends N75W and plunges west. To the west, near the San Miguelito amphitheater, the fold axis plunges east and trends more westerly. As the axis rises to the west, the underlying Padre Juan fault also rises, but does so more steeply than the fold axis, and in a west direction the north limb of the fold is truncated by the fault at progressively higher levels. Surface mapping shows a sub-parallel, left-stepped en echelon anticlinal axis originating approximately 275 m (900 ft) south of the truncated west end of the San Miguelito anticlinal axis and continuing west offshore.

The Rincon anticline is exposed at the surface north of the Javon Canyon/Padre Juan fault from Javon Canyon west into the Santa Barbara Channel. Onshore, the surface trace of the Rincon anticlinal axis is up to 300 m (985 ft) south of the subsurface trace at the "P" electric log horizon and below (Figs. 5F, 5G, 8). Where the divergence is greatest the subsurface anticlinal trace lies almost directly beneath the North syncline axis, a structure that parallels the Red Mountain fault at the surface, but does not extend downward to the "P" horizon. Dips on the limbs of the fold at the surface are much steeper than in the subsurface at the "P" horizon and the wavelength of the Rincon anticline-North syncline pair at the surface is considerably shorter than that of the subsurface anticline. This suggests a very shallow detachment between the surface and the "P" horizon.

The Rincon anticline in the subsurface plunges continuously to the east except at its eastern end where it is beneath the Padre Juan fault. There it broadens and rises to the east as it coalesces with the deep

Ventura Avenue anticline. The fold has a decreasing radius of curvature with increasing depth, and like the Ventura Avenue anticline to the east (Yeats, 1983), it may not extend beneath the ductile fine-grained Miocene strata of the Sisquoc Formation. It contains minor south-dipping reverse faults throughout, but only one north-dipping reverse fault is recognized (Fig. 5A).

At its eastern end, the north limb of the fold dips from 35° to 45° and is truncated by the Red Mountain fault. West of the saddle in the fold, the Rincon anticline strikes slightly more westerly than the Red Mountain fault (N70W vs. N65W), and west of Javon Canyon, north limb dips flatten at depth and eventually form a synclinal axis adjacent to the Red Mountain fault (Fig. 5G). This truncated syncline may be continuous with the North syncline seen offshore just west of the study area (see Jackson and Yeats, 1982), but it is not continuous with the surface trace of the North syncline in the study area.

The south limb of the Rincon anticline at the "Jc" horizon can be divided into two sections (Fig. 9A). From the east edge of the anticline to the San Miguelito amphitheater area, the crest of the structure is broad with south-southwest to west-southwest dips. Here the radius of curvature of the fold is 750 to 900 m (2500 to 3000 ft). South limb dips increase gradually with depth from 30° to 45° before being truncated by the Padre Juan fault. West of the San Miguelito amphitheater, the south limb of the Rincon anticline strikes more westerly than to the east. Additionally, at cross-section F-F' (Fig. 5C), the radius of curvature is only 180 m (600 ft) at the "Jc" horizon. This figure reduces to near 140 m (450 ft) at the west end of Rincon oil field. In the oil field, dips on the south limb of the fold steepen from 25° in the shallow subsurface to 45° at greater than -1500 m (-5000 ft). At depths greater than -3650 m (-12,000 ft), dips begin to flatten again. Dipmeter measurements below the Padre Juan fault in well 21 (Fig. 5D) indicate that beds take on a low north dip, thereby forming a deep synclinal axis beneath the fault. This syncline extends from south of the broadly folded portion of the Rincon anticline on the east for an unknown distance westward, and is here called the Rincon syncline.

Javon Canyon/Padre Juan Fault. The Padre Juan fault is the largest south-dipping reverse fault in the Ventura Avenue anticline-Rincon anticline trend. It separates the Rincon anticline below from the San Miguelito anticline above. The fault displaces Pico, Repetto, and Sisquoc strata and is best defined in the subsurface in the San Miguelito and eastern Rincon oil fields. As it shallows, the fault zone becomes increasingly broad and is referred to by industry geologists as the "zone of steep beds"--the top and base of which are mapped separately as the "top of steep beds" and the "base of steep beds". Repeat of microfossil zones in wells G-461 and G-415 (Fig. 5B) shows that major displacement occurs near the "base of steep beds". This displacement dies out rapidly northward due to folding above the fault surface. The Javon Canyon fault (Sarna-Wojcicki et al, 1979) is mapped at the surface from west of Javon Canyon to Padre Juan Canyon and inferred from subsurface mapping eastward to north of the San Miguelito amphitheater (Fig. 3). The Javon Canyon fault dips 60° to 75° south in the subsurface, extends downward near the "top of steep beds", and coalesces with the Padre Juan fault at depth (Fig. 6). Except where the Javon Canyon fault or the Padre Juan fault is explicitly referred to, the term Javon Canyon/Padre Juan fault is used to describe the fault system.

In the subsurface, the Padre Juan fault extends west from the Grubb fault through San Miguelito oil field and south of Rincon oil field, and then offshore where it is inferred from a dipmeter reversal in well 33 (Figs. 5G, 6). The fault dips 65° to 70° south where it is south of the hinge of the Rincon anticline, though dips are only 55° to 60° at San Miguelito oil field where the underlying Rincon anticline has a large radius of curvature. Evidence from well 21 (Fig. 5D) shows that the dip of the fault shallows below about -3950 m (-13,000 ft) in Repetto and/or Sisquoc strata, suggesting that the fault ramps upward from near the top of the Sisquoc Formation. As it impinges on the hinge of the Rincon anticline, the Padre Juan fault continues to cut stratigraphically up-section but bends over the anticlinal axis along the "base of steep beds". The strike of the fault south of the region where it flattens over the Rincon anticline axis is about N85W. This is sub-parallel to the strike of most of the other south-dipping faults found in the Ventura Avenue and San Miguelito oil fields, but it is more westerly than the strike of the Rincon anticline. The fault diverges away from the Rincon anticline in a westward direction and only the steeply dipping portion of the fault is preserved west of central Rincon oil field.

On the surface, the Javon Canyon/Padre Juan fault cuts Punta Gorda terrace deposits east of Javon Canyon at the well 16 drill site (Sarna-Wojcicki et al, 1979) (Fig. 3). In Javon Canyon, this fault cuts terrace alluvium graded to the 3500 year old Sea Cliff terrace platform (Sarna-Wojcicki et al, 1979; in press). The fault then disappears under the Sea Cliff terrace before reappearing on the ocean floor as a discontinuity in microfossil zones (Jackson, 1981). Surface evidence for the Javon Canyon fault east of the well 16 drillsite is questionable, although at one location east of Hill 1192 there is a near-vertical fault cutting Santa Barbara and/or Pico Formation strata. In the subsurface where the Javon Canyon fault is above the Padre Juan fault, it strikes about N85W and has a nearly planar south-dipping surface (see Javon Canyon fault contours in Figure 6). The Javon Canyon fault is a very young structure that cuts upward through the north limb of the San Miguelito anticline where the Padre Juan fault flattens over the axis of the Rincon anticline.

Maximum reverse separation on the Javon Canyon/Padre Juan fault occurs approximately 300 m (1000 ft) east of Padre Juan Canyon and is 2800 m (9200 ft) at the "middle" Pico-"lower" Pico contact. Stratigraphic separation for the same horizon is about 2450 m (8050 ft). Fault separation decreases rapidly eastward along strike (Fig. 9B), where in only 4 km (2.5 mi), reverse separation decreases to near 300 m (1000 ft) at the point where the Padre Juan fault encounters the northwest striking Grubb fault. In the northeast corner of San Miguelito oil field, electric log correlations suggest no significant faulting on the projection of the Padre Juan fault, only a zone of steeply north-dipping Plio-Pleistocene strata (Fig. 5A). Right-lateral motion on the Padre Juan fault, as suggested by Hsü (1977), is unlikely as it is difficult to envision significant lateral motion on the fault because it dies out so rapidly to the east and north.

Minor South-dipping Reverse Faults. Several south-dipping reverse faults with displacements generally less than 200 m (650 ft) cut both the San Miguelito and Rincon anticlines. All are subparallel to the anticlines they cut and most are constrained to the south limbs and hinge zones of the folds. Two of the larger, more continuous of these faults, the 2-S and 4-S, lie above the Javon Canyon/Padre Juan fault in San Miguelito oil field (Figs. 5B, 5C). The 4-S is approximately 600 m (2000 ft) above the Javon Canyon/Padre Juan fault at cross-section C-C' (Fig. 5B). It probably coalesces with the larger fault about 2.4 km (1.5 mi) farther west. To the east, it apparently dies out near cross-section A-A' (Fig. 5A). The 2-S fault lies about 400 m (1300 ft) above the 4-S. The 2-S fault extends from east of the northwest trending Grubb fault west past cross-section F-F' (Fig. 5C) where well control is absent. Both faults bend over the hinge of the San Miguelito anticline and die out northward where the overlying strata are folded above them. They also disappear into bedding at depth in the "lower" Pico and Repetto Formations. The 2-S fault may approach near enough to the surface to control the formation of the en echelon anticline seen south of the west end of the San Miguelito anticline (Fig. 3), though it could not be identified in well 23 (Fig. 5E) where this anticline occurs.

The 0-S fault, seen in the west face of the San Miguelito amphitheater (Fig. 10), cuts the San Miguelito anticline and is above the 2-S fault. It is found in the subsurface only in well 13 (Fig. 5B). The 0-S fault exposure provided the basis for the interpretation for most of the other south-dipping faults, including the Padre Juan, found in the study area. Detailed examination of the 0-S fault shows that either the fault must become a bedding plane feature in a north direction, or, more likely, that the strata above the fault must be tectonically overfolded in the hinge region of the overlying anticline for fault displacement to disappear completely to the north towards the Red Mountain fault.

Minor south-dipping faults in Rincon oil field, located within the Rincon anticline, are similar to, but strike more irregularly than faults in San Miguelito oil field. Only the A-4 fault, which extends from San Miguelito oil field into Rincon oil field (Figs. 5C-5F) for a distance of about 5.5 km (3.4 mi), is relatively easy to identify.

The south-dipping, east-northeast striking C-3 fault (also known as the Rincon Field fault) penetrated deep in the subsurface in western Rincon oil field (Figs. 5E, 5G, 6), possibly is a late Pleistocene structure. However, the fault trace mapped is highly speculative and data gathered for this study did not allow further investigation of the timing and significance of this fault.

KINEMATIC ANALYSIS OF LATE PLEISTOCENE TO RECENT DEFORMATION

Late Pleistocene Folding

The Ventura Avenue anticline separates westward into two structures near the Ventura Avenue-San Miguelito oil field boundary. Above the Padre Juan fault, the axis of the anticline is stepped right across the Grubb fault, west of which it is called the San Miguelito anticline. Formation of the San Miguelito anticline is closely related to the formation of the underlying Padre Juan fault. Below this fault, the Ventura Avenue anticline continues west as the Rincon anticline and is traced more than 20 km (12.5 mi) offshore to the west. In the south limb of the Ventura Avenue anticline at Ventura, the youngest steeply dipping Saugus Formation preserved beneath the moderately tilted Ventura marine terrace is approximately 200,000 years old (Lajoie et al, 1982). The Ventura Avenue anticline, therefore, began to form no more than 200,000 years ago. Because of the continuity and similarity of the Ventura Avenue anticline and the Rincon anticline, both structures are assumed to have begun to form at the same time.

The Ventura Avenue anticline contains many characteristics of a flexural-slip fold (Yeats, 1979; 1983): Dips along the flanks steepen with increasing depth, the radius of curvature of the fold hinge reduces with increasing depth until it becomes almost kink-like below -3650 m (-12,000 ft) in lower Repetto strata. The ratio of pore fluid pressure to lithostatic pressure varies inversely with the radius of curvature where radius of curvature values are less than about 300 m (1000 ft). Pore fluid pressure reaches 80 percent of lithostatic pressure at radius of curvature values of approximately 30 m (100 ft). The flattening and irregularity of dipmeter readings and the anomalously great thicknesses for the Sisquoc and Monterey Formations in the Shell, Taylor 653 deep test well (see Fig. 3 of Yeats, 1983), suggest that the Ventura Avenue anticline is a rootless fold above a major decollement in subjacent fine-grained, mechanically incompetent Miocene units. Many of the same conditions can be seen or inferred for the Rincon anticline.

Late Pleistocene folding of the Rincon anticline was complicated by the close proximity of the Red Mountain fault north of the anticlinal axis (cf. Fig. 5E,). The strands of the Red Mountain fault are planar and through-going, suggesting that deformation of the Plio-Pleistocene strata in the Ventura basin did not penetrate beyond the fault. The Red Mountain fault hanging wall block acted as a buttress that caused space problems for shortening associated with horizontal compression in the basin. Additionally, as shown above, the surface trace of the Rincon anticline is south of the subsurface trace of the same fold (Fig 8). Further, the North syncline occurs onshore at the surface north of the Rincon anticline axial trace, but it does not occur at depth. This disharmonically folded region is contained between opposing surfaces of the Red Mountain and the Javon Canyon/Padre Juan faults. It is above a shallow detachment surface that rises to the southwest near the top of sand-rich Pico Formation turbidites. Possibly rocks of the Red Mountain fault hanging wall block acted not only as a passive barrier at the north edge of the Ventura basin, but also rode up over, and displaced to the south, predominantly fine-grained Pleistocene strata in the basin north of the Javon Canyon/Padre Juan fault.

Rates of axial uplift relative to sea level for the last 200,000 years have been estimated for the Ventura Avenue anticline. Keller et al (1982) and Rockwell et al (1984) studied uplifted Ventura River terraces and showed uplift of the crest of the Ventura Avenue anticline to be 10.5 to 11.5 mm/yr (0.41 to 0.45 in/yr) for the period 80,000 to 30,000 years ago and 4.2 to 5.2 mm/yr (0.17 to 0.20 in/yr) for the last 30,000 years. Yeats (1979) extrapolated the 200,000 year old Saugus surface over the crest of the Ventura Avenue anticline. From this he determined an uplift rate for the last 200,000 years of 11 mm/yr (0.43 in/yr) and a tilt rate of 3.4 μrad/yr for the south limb of the fold. Subtracting out Keller et al's estimated uplift for the last 80,000 years from Yeats' value results in an uplift rate of 15 to 16 mm/yr (0.59 to 0.63 in/yr) for the period 200,000 to 80,000 years ago. [The progressive reduction of uplift rates is not indicative of a similar reduction of shortening rates across the northern Ventura basin. A rootless fold formed by lateral compression would initially experience high uplift rates which would gradually reduce as folding continued at a constant shortening rate (Currie et al, 1962; Adams, 1984).]

Uplift rates for the Punta Gorda and Sea Cliff terraces due to Rincon anticline folding cannot be determined accurately because the uplift is complicated by Javon Canyon/Padre Juan faulting and San Miguelito anticline folding and by the disharmonic folding that occurred above the shallow detachment in Rincon oil field. Subsurface mapping, however, allowed structural relief due to folding to be determined and the long term fold rate for the anticline to be estimated. At cross-section J-K' (Fig. 7A), there are 1580 m (5200 ft) of structural relief on the "lower" Pico-Repetto contact between the crest of the Rincon anticline and the trough of the Rincon syncline beneath the Padre Juan fault. There are 640 m (2100 ft) of structural relief on the "lower" Pico-Repetto contact between the crest of the

Rincon anticline and the south end of cross-section J-K' above the Padre Juan fault. Uplift due to folding on the Rincon anticline is considerably less than for the Ventura Avenue anticline at Ventura where there are no late Pleistocene faults with displacements as large as the Javon Canyon/Padre Juan fault. There, structural relief between the fold axis and the basin plain at the "lower" Pico-Repetto contact approaches 3050 m (10,000 ft). For the Rincon anticline at cross-section J-K', assuming the Pico Formation "P" horizon to have been flat lying 200,000 years ago, the maximum tilt rate for the south limb of the fold is 3.1 μrad/yr. Pre-200,000 year old basin flexure and subsidence and evidence for early Pleistocene uplift at the north edge of the basin suggest a more realistic tilt rate of less than 3.0 μrad/yr.

At cross-section J-K', the amount of shortening at the "middle" Pico-"lower" Pico contact due to folding of the Rincon anticline was determined to be 975 m (3200 ft). Shortening was measured perpendicular to the strike of the anticline. Points of pinning were South Strand 1 of the Red Mountain fault and the Padre Juan fault. The estimated rate of shortening due to Rincon anticline folding for the last 200,000 years is at least 4.9 mm/yr (0.19 in/yr). (See Table 2 for a summary of the late Pleistocene to Holocene shortening that has occurred across the Ventura basin along cross-section J-K'.)

Table 2: Individual components and rates of Plio-Pleistocene shortening determined along cross-section J-K' (Fig. 7) and cross-section II (Fig. 12). See text for discussion of time and rate of deformation for Red Mountain fault and Red Mountain anticline. Datum refers to the horizon on which shortening was determined. ⁂5 is the 1.0 Ma horizon of Yeats (1981). PJF/SMA, Padre Juan fault/San Miguelito anticline.

TABLE 2: VENTURA BASIN SHORTENING ALONG CROSS-SECTION J-K' AND CROSS-SECTION II

Location (Datum)	Total Shortening [m (ft)]	Assumed Shortening Last 0.2 Ma [m (ft)]	0.2 Ma Shortening Rate [mm/yr (in/yr)]
Santa Barbara Channel (&5)	1300 (4300)	0-1300 (0-4300)	0.0- 6.5 (0.00-0.25)
PJF/SMA (Top/L. Pico)	1525 (5000)	1525 (5000)	7.6 (0.30)
Rincon Anticline (Top/L. Pico)	975 (3200)	975 (3200)	4.9 (0.19)
Red Mtn. Fault (Top/Sisquoc)	2925 (9600)	0- 430 (0-1480)	0.0- 2.3 (0.00-0.09)
Red Mtn. Anticline (Top/Sisquoc)	1100 (3600)	0- 170 (0- 550)	0.0- 0.9 (0.00-0.03)
Totals	7825 (25700)	2500-4400 (8200-14530)	12.5-22.3 (0.49-0.87)

Javon Canyon/Padre Juan Faulting and San Miguelito Anticline Folding

Although the tendency of the Padre Juan fault is to bend over the axis of the underlying Rincon anticline, a synchronous relation for faulting and folding must be considered. First, there appears to be no change of thickness of units across the fault, thereby constraining all motion on the fault to later than deposition of the youngest units involved in faulting. Second, like all other south-dipping faults within the fold, the Padre Juan fault tends to die out over the axis of the Rincon anticline. That the locus of the underlying fold would be located where these faults begin to die out is possible, but not likely, because of the larger scale continuity of the folds compared to the faults in the anticlinal trend. Finally, the structural geology in cross-section J-K' (Fig. 7A), requires synchronous faulting and folding: Restoration of Repetto and Pico Formation strata above the Padre Juan fault in order to evaluate the timing and extent of the Rincon syncline does not reflect the formation of a pre-fault fold. The sub-fault syncline apparently formed by progressive flattening of the lower part of the fault surface (from X to Y in Figs. 7A and 7B) as faulting proceeded. This process, and the formation of the Rincon anticline during faulting, resulted in increasingly greater northward translation of the Padre Juan fault surface at progressively deeper levels.

Williams and Chapman (1983), Suppe and Medwedeff (1984) and Suppe (1985) discuss a process called fault-propagation folding by Suppe whereby an asymmetric hanging wall fold grows above the leading edge of a thrust fault in response to ongoing lateral compression. The folding above the fault allows progressively larger displacements back from the fault tip. The fault tip itself is propagated forward most often in the asymmetric synformal axis formed in front of the growing anticline. In this manner propagation of the leading edge of the fault is a consequence of the growth of the fold--rather than folding being a consequence of faulting as is the case with fault-bend folding (cf. Rich, 1934; Rodgers, 1950). Compare Figure 11B with 11A.

The relationship of the San Miguelito anticline to the Padre Juan fault is complicated by the underlying Rincon anticline and by the northern abutment caused by the structurally and topographically high hanging wall block of the Red Mountain fault. The conspicuous "zone of steep beds" on the north limb of the San Miguelito anticline, however, indicates that fault-propagation folding may have been the process controlling the early formation of the fault-anticline pair, especially since propagation of the Padre Juan fault northward is at or

Figure 11: A) Idealized example of a fault-bend fold. Folds are constrained to the hanging wall of the fault and result from bends in the underlying fault surface. From Suppe (1985). B) Idealized example of a fault propagation fold. Folding occurs at the tip of the growing fault surface. As the fault tip propagates forward in the core of the steeply dipping to overfolded syncline, the fold grows increasingly larger. From Suppe (1985). C) Idealized example of a fault-propagation fold underlain by a simultaneously active fold. This idealized figure was produced by sequence of events which may have formed the Javon Canyon/Padre Juan fault-San Miguelito anticline pair above the Rincon anticline. D) Simplified cross-section incorporating F-F' (Fig. 5C) and illustrating the similarity of this case with the idealized example shown in C, above.

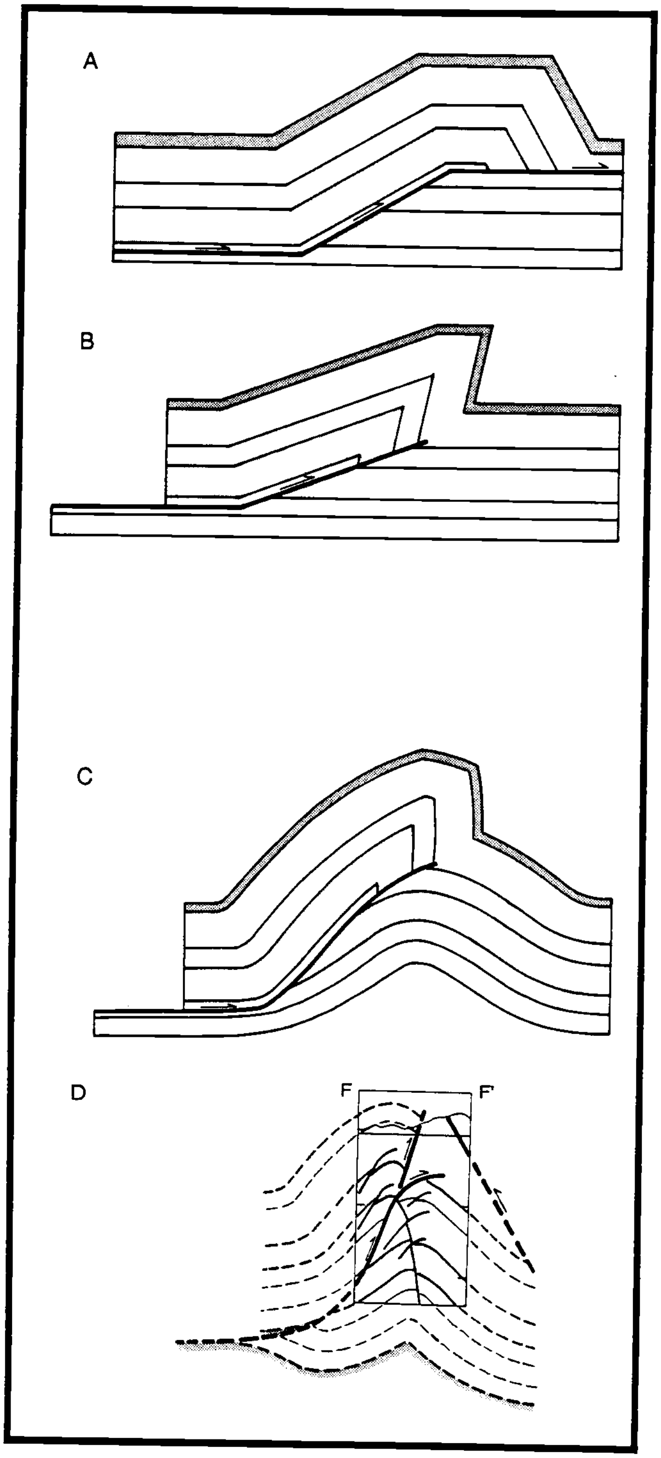

Figure 11.

near the base of the "steep beds" on the north limb of the San Miguelito anticline (Figs. 5B, 11C, 11D). Additionally, the fault dies out northward and does not penetrate any strands of the Red Mountain fault. The rapid reduction of displacement is partially accommodated by the overlying folding. Further accommodation of the excessive lateral shortening above the Padre Juan fault and of the loss of displacement over the axis of the Rincon anticline is accomplished by late stage faulting, exemplified by the Javon Canyon fault, which cuts upward near the "top of steep beds".

Restoration of cross-section J-K' (Fig. 7B) allowed shortening for the last 200,000 years south of the Padre Juan fault at the "middle" Pico-"lower" Pico contact to be calculated. The 1525 m (5000 ft) of shortening determined represents combined shortening due to Javon Canyon/Padre Juan faulting and San Miguelito anticline folding. It also accounts for any shortening south of the fault trace incurred by pre-fault folding of the Rincon anticline--though where the Javon Canyon/Padre Juan fault is largest, there may have been no appreciable pre-fault folding. The rate of shortening due to combined faulting and folding for the last 200,000 years is 7.6 mm/yr (0.30 in/yr).

Cross-section K-K' (Fig. 5E) contains the well 16 drill site where 42 to 49 m (138 to 160 ft) of south-side up Javon Canyon fault offset of 45,000 to 50,000 year old Punta Gorda terrace deposits was measured (Sarna-Wojcicki et al, 1979; in press). 750 m (2500 ft) west of that location, 4 m (13 ft) of south-side up displacement of terrace debris graded to a 3500 year old Sea Cliff terrace platform was identified (Sarna-Wojcicki et al, in press). These offsets give uplift rates of 0.9 to 1.1 mm/yr (0.037 to 0.044 in/yr) and 1.1 mm/yr (0.044 in/yr) for the last 45,000 to 50,000 years and 3500 years, respectively. Recalculation of these values to determine horizontal shortening across a 60° south-dipping fault plane gives rates of shortening of 0.45 to 0.55 mm/yr (0.019 to 0.022 in/yr) for the last 45,000 to 50,000 years, and 0.55 mm/yr (0.022 in/yr) for the last 3500 years. Both values fall far short of the 200,000 year rate of 7.6 mm/yr (0.30 in/yr) determined from subsurface measurements on the "middle" Pico-"lower" Pico contact across the Javon Canyon/Padre Juan fault. Tectonism in the basin may have been reduced since the terrace benches were cut. However, it is also reasonable that 1) the Javon Canyon is one of a number of faults in the hanging wall of the Padre Juan fault and its shortening rate is not representative of the total shortening occurring across the system, and 2) the Javon Canyon fault is not favorably oriented for easy or rapid dip-slip motion, therefore, the greatest shortening currently taking place is by folding above the Padre Juan fault.

Late Pleistocene Shortening Due to Red Mountain Faulting and Folding

The Red Mountain fault system differs from the late Pleistocene Ventura basin structures already discussed: it began to form earlier, it is deep-seated and offsets pre-Miocene sedimentary rocks and probably basement, it is seismically active (Yeats et al, in press), and geologic conditions before and during initial motion are not well constrained.

There is considerable displacement across the faulted zone in the study area: at cross-section J-K' (Fig. 7A), 5850 m (19,200 ft) of reverse separation of the Repetto-Sisquoc contact was estimated; up to 7300 m (23,900 ft) of reverse separation of the same contact was estimated at cross-section C-C' (Fig. 5B). Jackson and Yeats (1982) suggest that initial motion on the Red Mountain reverse fault system occurred during deposition of lower Santa Barbara strata, though there is no direct evidence that confirms this. Not all reverse separation may be Pleistocene and Holocene, however. Because Red Mountain was a seaknoll during the Pliocene (Yeats et al, in press), an ancestral high-angle Red Mountain fault with north-side-up separation may have existed since the deposition of lower Repetto or upper Sisquoc strata into the basin. Possibly, the present high-angle reverse faults of the Red Mountain fault system may be reactivated structures that correspond to, or precede, the thinning and fining of Pliocene strata towards the Red Mountain seaknoll.

To determine deformation rates across the Red Mountain fault, the onset of reverse motion was estimated to be between 2.4 Ma ago [the approximate age of the Repetto-Sisquoc contact (Repettian-Delmontian stage boundary) in the Ventura area (Dickinson et al, in press)] and 1.3 Ma ago [the time of initiation of motion on the Taylor fault set (Yeats, 1979; 1983) and the approximate age of the base of the Santa Barbara Formation "Mud Pit shale" in the north half of Rincon oil field]. For the 55° north dipping faults measured in cross-section C-C', this gives a reverse separation rate of 3.0 to 5.6 mm/yr (0.12 to 0.22 in/yr), a vertical separation rate of 2.5 to 4.6 mm/yr (0.10 to 0.18 in/yr), and a shortening rate of 1.7 to 3.2 mm/yr (0.07 to 0.13 in/yr) for the last 2.4 to 1.3 Ma. Similarly, for the 60° north-dipping faults measured in cross-section J-K', the reverse separation rate is 2.4 to 4.5 mm/yr (0.10 to 0.18 in/yr), the vertical separation rate is 2.1 to 3.9 mm/yr (0.08 to 0.15 in/yr), and the shortening rate is 1.2 to 2.3 mm/yr (0.05 to 0.09 in/yr) for the last 2.4 to 1.3 Ma. The vertical separation rates determined above are larger than the 0.5 to 1.6 mm/yr (0.019 to 0.062 in/yr) rates attained across offset Punta Gorda terrace deposits for the last 45,000 to 50,000 years (Sarna-Wojcicki et al, 1979, Jackson and Yeats, 1982). Because not all Holocene motion across the strands of the Red Mountain fault system may yet be accounted for and because geodetic surveys carried out along the Ventura River between the years 1934 and 1968 show 3.7 mm/yr (0.15 in/yr) differential movement across the fault (Buchanan-Banks et al, 1975), the long-term 1.2 to 2.3 mm/yr (0.05 to 0.09 in/yr) rate of shortening measured at cross-section J-K' may be a reasonable rate for the last 200,000 years.

Jackson and Yeats (1982), however, suggest that separation rates for the Red Mountain fault have not been constant throughout the Quaternary. For that reason, only broad constraints were placed on Red Mountain fault shortening rates used to determine basin shortening for the last 200,000 years. The juxtaposition of "upper" Pico (Santa Barbara ?) shales against the Red Mountain fault at depths greater than -2500 m (-8200 ft) (Fig. 5B), indicates significant motion on the Red Mountain fault since the beginning of Santa Barbara Formation deposition. The 2.3 mm/yr (0.09 in/yr) maximum rate arrived at in Table 2 for shortening due to Red Mountain faulting considered all offset of the top Sisquoc horizon to have occurred at a constant rate since the onset of Santa Barbara deposition roughly 1.3 Ma ago. Seismicity and offset late Pleistocene marine terraces are direct evidence that the Red Mountain fault is still active. The minimum uplift rate of faulted Punta Gorda terrace deposits is 0.5 mm/yr (0.019 in/yr). For a 60° dipping fault plane this translates into a 0.3 mm/yr (0.011 in/yr) shortening rate for the last 45,000 to 50,000 years. However, since no other evidence exists requiring greater displacement on the Red Mountain fault for the last 200,000 years, negligible shortening for the last 200,000 years had to be assumed as the minimum value in Table 2.

Assuming the Red Mountain anticline to have formed during Red Mountain reverse faulting permitted deformation rates at and beyond the north end of cross-section J-K' to be estimated. The top Sisquoc datum was extrapolated northward over the Red Mountain anticline from its contact with North Strand 1 of the Red Mountain fault to the Ayers Creek syncline to obtain 1100 m (3600 ft) of shortening (Figs. 1, 12). Using similar reasoning as above, the shortening rate due to folding of the Red Mountain anticline was estimated to be between 0.0 and 0.9 mm/yr (0.0 and 0.03 in/yr) for the last 200,000 years.

Figure 12: Regional cross-section II. Shown in Figure 1. See Figure 3 for legend. Section incorporates cross-section J-K' (Fig. 7A). Geology shown south of J-K' is adapted from Yeats (1981). Horizontal contraction south of J-K' is determined along &5, a regional 1.0 Ma chronostratigraphic horizon. ACS, Ayers Creek syncline; JC/PJF, Javon Canyon/Padre Juan fault; RA, Rincon anticline; RMA, Red Mountain anticline; RS, Rincon syncline; SMA, San Miguelito anticline.

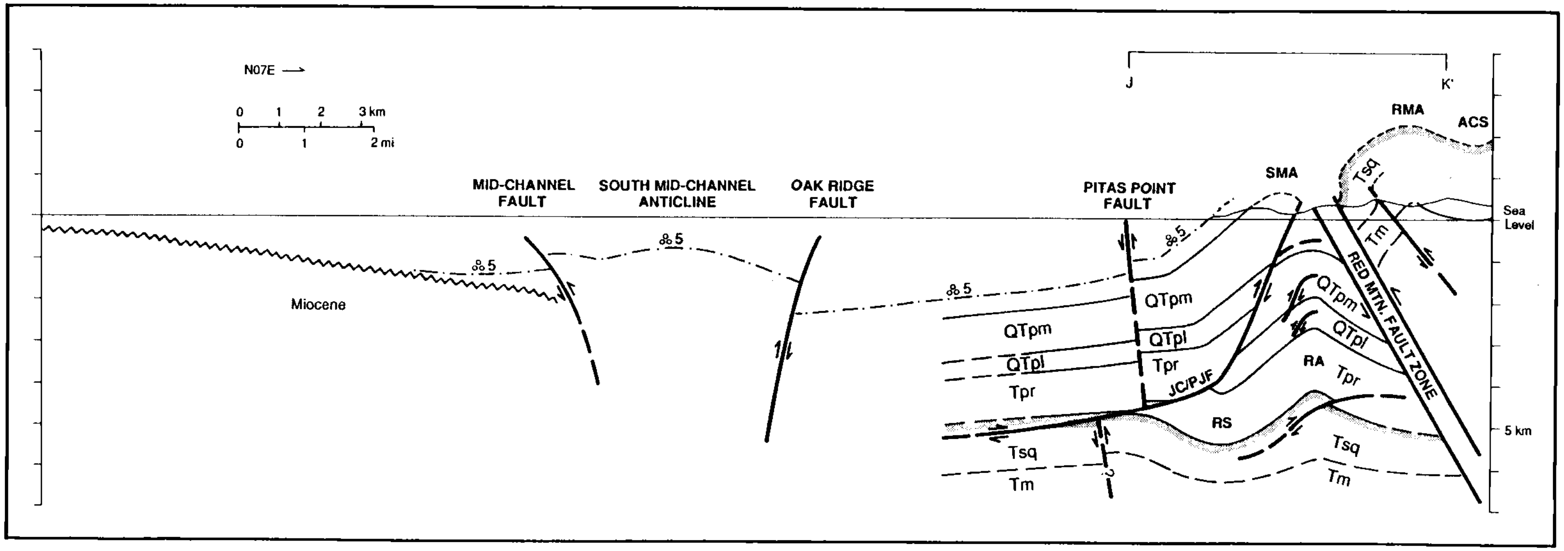
N07E
0 1 2 3 km
0 1 2 mi
MID-CHANNEL FAULT
SOUTH MID-CHANNEL ANTICLINE
OAK RIDGE FAULT
PITAS POINT FAULT
J
K'
SMA
RMA
ACS
Sea Level
5 km
Miocene
QTpm
QTpl
Tpr
Tsq
Tm
JC/PJF
RA
RS
RED MTN. FAULT ZONE

Figure 12.

CONCLUSIONS

The structural evolution of the area of the northern Ventura basin encompassing the Rincon and San Miguelito oil fields involves a short, but complex, history. The deposition of the latest Oligocene to early Miocene Vaqueros Formation basal transgressive sandstone and of the overlying shales of the Rincon, Monterey, and Sisquoc Formations signaled the onset and maturation of a rapid basin-forming event in the southern California Borderland region (Natland, 1957; Ingle, 1980; Dickinson et al, in press). In the northern Ventura basin, this sequence is overlain by up to 4000 m (13,000 ft) of Pliocene and Pleistocene Repetto and Pico Formation turbidites. These strata were deposited at sedimentation rates of up to 2.0 mm/yr (0.08 in/yr) (Ingle, 1980) into a basin subsiding at 1.5 mm/yr (0.06 in/yr) (Yeats, 1978). Cessation of high subsidence rates during the time of Santa Barbara "Mud Pit shale" deposition was followed by renewed rapid subsidence and accumulation of Saugus Formation marine and nonmarine deposits east of the study area. The nature of the boundary that developed during the formation of the northern Ventura basin is not well understood because no Plio-Pleistocene strata are preserved north of the basin-bounding Red Mountain fault system until that system cuts into basin to the west in the Santa Barbara Channel. In the study area, the Sisquoc Formation is the only formation observed both in the Ventura basin and north of the Red Mountain fault system.

The prominent structures in the study area formed as a result of rapid Pleistocene to Holocene tectonism. The Red Mountain fault, which forms the northern boundary of the Ventura basin, may have also been active in the Pliocene. Evidence for thinning and fining of upper Sisquoc, Repetto, and Pico Formation strata towards the fault in the Red Mountain area infer possible activity since at least early Pliocene time. The Red Mountain fault zone, now seen as a steeply north-dipping tectonic boundary, may be a reactivated system that broke along earlier high-angle faults that formed the south side of a Pliocene seaknoll in the Red Mountain area (Yeats et al, in press). 5850 m (19,200 ft) of reverse separation of the Repetto-Sisquoc contact was estimated across the Red Mountain fault zone at cross-section J-K' (Fig. 7A). The amount of displacement that occurred prior to the Pleistocene is unknown, though much of the reverse motion on the fault probably occurred in the last 1.3 Ma. This corresponds approximately with the time of the upward change from Pico Formation turbidites to the Santa Barbara Formation "Mud Pit shale" in the northern part of the basin. At Ventura, the transition upwards to the

"Mud Pit shale" is clearly conformable and transitional. In the study area the change is more complex: It occurred later on the east than the west and it may be an unconformity surface that was subsequently faulted. 1.2 Ma old Bailey ash and Santa Barbara Formation microfauna occurrences in the shale preclude it from being a block of older fine-grained strata faulted up from depth.

The major structures in the Ventura basin in the study area began to form long after the Red Mountain reverse fault system became active. Evidence east of the field area indicates the Ventura Avenue anticline is no more than 200,000 years old (Lajoie et al, 1982; Yeats, 1983). Beneath the intersection of the Grubb and Padre Juan faults, the deep Ventura Avenue and Rincon anticlines are a continuous structure. Since the Ventura Avenue anticline is the more severely folded of the two, the Rincon anticline is probably no older than the Ventura Avenue anticline. The Javon Canyon/Padre Juan fault, the largest south-dipping reverse fault in the anticlinal trend with up to 2800 m (9200 ft) of reverse separation, is also no older than 200,000 years. Though the fault everywhere flattens over the axis of the underlying Rincon anticline, it does not predate the fold because flattening always corresponds with the loss of separation across the fault. Also, when restored to its pre-fault condition, the structural geology above the

Padre Juan fault in cross-section J-K' is not compatible with the existence of an older, well developed Rincon syncline beneath the fault. The San Miguelito anticline, formed in the hanging wall of the Padre Juan fault and having a steeply dipping to overfolded north limb, is directly related to the fault and is interpreted as a fault-propagation fold. The San Miguelito anticline is a complex example, however, because the hanging wall block of the Red Mountain fault acted as a buttress against which basin shortening was directed and because concurrent growth of the Rincon anticline occurred beneath the Padre Juan fault. The Javon Canyon fault is a significant late stage splay of the Padre Juan fault that extends upwards to the surface above the Padre Juan fault where that fault flattens over the axis of the Rincon anticline.

Historic seismicity attributed to the Red Mountain fault and the presence of elevated and faulted marine terraces varying in age from 105,000 years to 1800 years indicate Ventura basin deformation is ongoing. The Javon Canyon fault offsets both 45,000 to 50,000 year old Punta Gorda and 3500 year old Sea Cliff terrace deposits near Javon Canyon (Sarna-Wojcicki et al, 1979; in press), while strands of the Red Mountain fault offset Punta Gorda and older terrace benches in the Javon Canyon and Los Sauces Creek areas (Geotechnical Consultants, 1968;

Sarna-Wojcicki et al, 1979).

Constraining the initiation of deformation to 200,000 years ago for the late Pleistocene structures in the Ventura basin in the study area allowed the rate of shortening across the study area for the last 200,000 years to be estimated. Table 2 summarizes total shortening for the Ventura basin along and beyond the cross-section J-K' (i.e. along cross-section II; Figs. 1, 12). The structural geology of the 1.0 Ma datum (∴5) from Yeats (1981) was used to estimate shortening for the portion of cross-section II south of J-K'. Though much of the 1300 m (4300 ft) of horizontal contraction measured probably occurred in the last 200,000 years, there is no evidence proving that to be the case. The rates shown in Table 2 for shortening south of cross-section J-K', therefore, reflect calculations for all and none of the shortening having occurred in the last 200,000 years.

Overall, there has been about 7825 m (25,700 ft) of north-south directed horizontal contraction across the Ventura basin along and beyond cross-section J-K' in the last 2.4 to 1.3 Ma. This shortening of upper crustal strata took place between the northern Channel Islands on the south and the Ayers Creek syncline on the north. Of this shortening, about 2500 to 4400 m (8200 to 14,530 ft) occurred in the last 200,000 years, resulting in a rate of shortening of 12.5 to 22.3 mm/yr (0.49 to 0.87 in/yr) since that time. As a comparison, at Ventura, Yeats (1981, 1983) determined the rate of north-south directed shortening along cross-section III (Fig. 1) for the last 200,000 years to be 23 mm/yr (0.91 in/yr), with almost ninety percent of that value resulting from the formation of the Ventura Avenue anticline.

Shortening rates found in the study area agree well with the trend established by Yeats (1981, 1983) of decreasing lateral contraction from east to west across the Ventura basin for the last 200,000 years (cross-sections I, III, and IV in Fig. 1; Table 3). For total shortening across the basin over the last 1.0 to 2.4 Ma, however, more shortening has occurred east and west of Ventura, than at Ventura [7800 m (25,600 ft) along cross-section II and 11,600 ± 2000 m (38,050 ± 6500 ft) along cross-section IV, vs. 5500 m (18,050 ft) along cross-section III]. Both in the study area (cross-section II), and at Fillmore (cross-section IV), where there is the greatest shortening, the majority of the pre-200,000 year old deformation was concentrated along the basin-bounding Red Mountain and San Cayetano reverse fault systems. These faults die out towards Ventura, and no large basin-bounding faults are identified at the north edge of the basin north-northeast of Ventura (cross-section III). This suggests that prior to 200,000 years ago, most

Table 3: Comparison of Plio-Pleistocene shortening that has occurred across the central and western Ventura basin. Values for cross-sections I, III, and IV (Fig. 1) were determined by Yeats (1981, 1983). Values for cross-section II are from this study.

TABLE 3: SHORTENING ACROSS CENTRAL AND WESTERN VENTURA BASIN

Cross-section Location	Sta. Barbara (I)	Rincon Oil Field (II)	Ventura (III)	Fillmore (IV)
Datum	&5	&5; T/Lower Pico; T/Sisquoc	&5	&5
Total shortening [m (ft)]	1800 (5900)	7825 (25,700)	5500 (18,050)	11,600±2000 (38,050±6560)
Shortening in Last 0.2 Ma [m (ft)]	0-1800 * (0-5900)	2500-4400 (8200-14,530)	4900 (16,100)	5000 # (16,400)
Pre-0.2 Ma Shortening [mm/yr (in/yr)]	< 1800 * (< 5900)	3425-5325 (11,170-17,500)	600 (1950)	6600±2000 # (21,650±6560)
0.2 Ma Shortening Rate [mm/yr (in/yr)]	0.0-9.0 * (0.00-0.35)	12.5-22.3 (0.49-0.87)	23 (0.91)	25 # (1.0)

* No direct evidence is known which allows shortening for last 0.2 Ma to be determined.

\# These amounts based on Yeats' (1983) assertion that shortening for last 0.2 Ma along this section should be similar to that for Ventura.

shortening apparently took place external to the Ventura basin. In the last 200,000 years, however, shortening rates in the Ventura basin have increased greatly (Table 3), and the Plio-Pleistocene strata in the basin have become involved in a rapid contractile deformational episode reflecting the effects of north-south directed compressive tectonic stresses. If this is so, it calls into question the view that the compressive deformation seen in the western Transverse Ranges is entirely due to forces originating at the constraining Big Bend of the San Andreas fault northwest of the study area. Rather, convergence of the Pacific plate northward against a mini-plate bounded by the San Andreas fault and the north-dipping reverse faults which define north edge of the Ventura basin, as suggested by Weldon and Humphreys (in press), must be considered.

REFERENCES CITED

Adams, J. 1984, Active deformation of the Pacific Northwest continental margin: Tectonics, v. 3, p. 449-472.

Bandy, O., 1960, The geological significance of coiling ratios in the foraminifer Globigerina pachyderma (Ehrenberg): Journal of Paleontology, v. 34, p. 671-681.

Buchanan-Banks, J. M., R. O. Castle, and J. I. Ziony, 1975, Elevation changes in the central Transverse Ranges near Ventura, California: Tectonophysics, v. 29, p. 113-125.

Currie, J. B., H. W. Patnode, and R. P. Trump, 1962, Development of folds in sedimentary strata: GSA Bulletin, v. 73, p. 655-674.

Dibblee, T. W., Jr., 1966, Geology of the central Santa Ynez Mountains, Santa Barbara County, California: California Division of Mines and Geology Bulletin 186, 99 p.

Dickinson, W. R., R. A. Armin, N. Beckvar, T. C. Goodlin, S. U. Janecke, R. A. Mark, R. D. Norris, G. Radel, and A. A. Wortman, in press, Geohistory analysis of rates of sediment accumulation and subsidence for selected California basins: UCLA Rubey Colloquium, Volume 6.

Geotechnical Consultants, Inc., 1968, Geotechnical investigation of proposed access road and process facilities, Mobil Oil Company's Rincon shore facility, Ventura County, California: Engineering Geology Reports, April 15, 1968; July 26, 1968; August 22, 1968; September 30, 1969.

Greene, H. G., S. C. Wolf, and K. H. Blom, 1978, The marine geology of the eastern Santa Barbara Channel with particular emphasis on the ground water basins offshore from the Oxnard Plain, southern California: U. S. Geological Survey-Open File Report 78-305, 104 p.

Hacker, R. N., 1970, Ventura Avenue oil field: in Ventura Avenue and San Miguelito Oil Fields: Pacific Section of American Association of Petroleum Geologists Field Trip Guidebook.

Hsü, K. J., 1977, Studies of Ventura field, California, I: Facies geometry and genesis of lower Pliocene turbidites: AAPG Bulletin, v. 61, p. 137-168.

______ K. Kelts, and J. W. Valentine, 1980, Resedimented facies in Ventura basin, California, and model of longitudinal transport of turbidity currents: AAPG Bulletin, v. 64, p. 1034-1051.

Ingle, J. C., 1967, Foraminiferal biofacies variation and the Miocene-Pliocene boundary in southern California: Bulletins of American Paleontology, v. 52, p. 217-394.

______ 1980, Cenozoic paleobathymetry and depositional history of selected sequences within the southern California Continental Borderland: Cushman Foundation for Foraminiferal Research, Special Publication 19, p. 163-195.

Izett, G. A., C. W. Naeser, and J. D. Obradovich, 1974, Fission track age of zircon from an ash bed in Pico Formation (Pliocene-Pleistocene) near Ventura, California: GSA Abstracts with Programs, v. 6, p. 197.

Jackson, P. A., 1981, Structural evolution of Carpinteria basin, western Transverse Ranges, California: M. S. thesis, Oregon State University, 93 p.

______ and R. S. Yeats, 1982, Structural evolution of Carpinteria basin, western Transverse Ranges, California: AAPG Bulletin, v. 66, p. 805-829.

Kaufman, A., W. S. Broecker, T. L. Ku, and D. L. Thurber, 1971, The status of U-series methods of mollusk dating: Geochem. Cosmochem. Acta, v. 35, p. 1155-1183.

Keller, E. A., T. K. Rockwell, M. N. Clark, G. R. Dembroff, and D. L. Johnson, 1982, Tectonic geomorphology of the Ventura, Ojai, and Santa Paula areas, western Transverse Ranges, California: in GSA Cordilleran Section Field Trip Guidebook, p. 25-42.

Kleinpell, R. M., 1938, Miocene stratigraphy of California: AAPG, 450 p.

Lajoie, K. R., J. P. Kern, J. F. Wehmiller, G. L Kennedy, S. A. Mathieson, A. M. Sarna-Wojcicki, R. F. Yerkes, and P. F. McCrory, 1979, Quaternary marine shorelines and crustal deformation, San Diego to

Santa Barbara, California: in P. L. Abbott, ed., Geological excursions in the southern California area: San Diego State University Department of Geological Sciences, p.3-15.

______ A. M. Sarna-Wojcicki, and R. F. Yerkes, 1982, Quaternary chronology and rates of crustal deformation in the Ventura area, California: in GSA Cordilleran Section Field Trip Guidebook, p. 43-51.

Liddicoat, J. C., and N. D. Opdyke, 1981, Magnetostratigraphy of Quaternary deposits in the Ventura basin of southern California to improve the dating of four important tephra units: in J. C. Ingle, ed., Pliocene/Pleistocene boundary in the southwestern United States: INQUA International Field Conference Guidebook, p. 11-22.

Luyendyk, B. P., M. J. Kamerling, and R. Terres, 1980, Geometric model for Neogene crustal rotations in southern California: GSA Bulletin, v. 91, p. 211-217.

Natland, M. L., 1952, Pleistocene and Pliocene stratigraphy of southern California: Ph.D. thesis, University of California, Los Angeles, 165 p.

______ 1957, Paleoecology of west coast Tertiary sediments: in H. S. Ladd, ed., Treatise on marine ecology and paleoecology: GSA Memoir 67, v. 2, p. 543-571.

Paschall, R. H., 1954, Geology of the Rincon oil field, Ventura County: in Geology of southern California: California Division of Mines and Geology Bulletin 170, Map Sheet 26.

Putnam, W. C., 1942, Geomorphology of the Ventura region: GSA Bulletin, v. 53, p. 691-754.

Rich, J. L., 1934, Mechanics of low-angle overthrust faulting as illustrated by Cumberland thrust block, Virginia, Kentucky, and Tennessee: AAPG Bulletin, v. 18, p.1584-1596.

Rockwell, T. K., E. A. Keller, M. N. Clark, and D. L. Johnson, 1984, Chronology and rates of faulting of Ventura River terraces, California: GSA Bulletin, v. 95, p. 1466-1474.

Rodgers, J., 1950, Mechanics of Appalachian folding as illustrated by Sequatchie anticline, Tennessee and

Alabama: AAPG Bulletin, v. 34, p. 672-681.

Sarna-Wojcicki, A. M., K. R. Lajoie, S. W. Robinson, and R. F. Yerkes, 1979, Recurrent Holocene displacement on the Javon Canyon fault, rates of faulting, and regional uplift, western Transverse Range, California: GSA Abstrcts with Programs, v. 11, p. 125.

______ H. R. Bowman, C. E. Meyer, P. C. Russell, M. J. Woodward, G. McCoy, J. J. Rowe, Jr., P. A. Baedecker, F. Asaro, and H. Michael, 1984, Chemical analyses, correlations, and ages of upper Pliocene and Pleistocene ash layers of east-central and southern California: U. S. Geological Survey Professional Paper 1293, 38 p.

______ K. R. Lajoie, and R. F. Yerkes, in press, Recurrent Holocene displacement of the Javon Canyon fault: a comparison of fault movement history with calculated average recurrence intervals: in U. S. Geological Survey Professional Paper 1339.

Suppe, J., 1985, Principles of Structural Geology: Prentice-Hall, Englewood Cliffs, NJ, 537 p.

Suppe, J., and D. A. Medwedeff, 1984, Fault-propagation folding: GSA Abstracts with Programs, v. 16, p. 670.

Weber, F. H., Jr., G. B. Cleveland, J. E. Kahle, E. F. Kiessling, R. V. Miller, M. F. Mills, D. M. Morton, and B. A. Cilweck, 1973, Geology and mineral resources study of southern Ventura County, California: California Division of Mines and Geology, Preliminary Report 14, 102 p.

Wehmiller, J. F., K. R. Lajoie, A. M. Sarna-Wojcicki, R. F. Yerkes, G. L. Kennedy, T. A. Stephens, and R. F. Kohl, 1978, Amino-acid racemization dating of Quaternary mollusks, Pacific Coast, United States: in R. E. Zartman, ed., Short papers of the fourth international conference, geochronology, cosmochronology, isotope geology: U. S. Geological Survey Open-File Report 78-701, p. 445-445.

Weldon, R., and E. Humphreys, in press, A kinematic model of southern California: Tectonics

Williams, G., and T. Chapman, 1983, Strains developed in the hangingwall of thrusts due to their slip/propagation rate: a dislocation model:

Journal of Structural Geology, v. 5, p. 563-571.

Woodring, W. P., R. Stewart, and R. W. Richard, 1940, Geology of the Kettleman Hills oil field, California: U. S. Geological Survey Professional Paper 195, 170 p.

Yeats, R. S., 1978, Neogene acceleration of subsidence rates in southern California: Geology, v. 6, p. 456-460.

______ 1979, Neotectonics of the Ventura Avenue anticline, semi-annual technical report, contract 14-08-0001-17730: U. S. Geological Survey, Menlo Park, California, 24 p.

______ 1981, Deformation of a 1 Ma datum, Ventura basin, California, final report, contract 14-08-0001-18283: U. S. Geological Survey, Menlo Park, California, 17 p.

______ 1982, Low shake faults of the Ventura basin, California: in GSA Cordilleran Section Field Trip Guidebook, p. 2-14.

______ 1983, Large-scale Quaternary detachments in Ventura basin, southern California: Journal of Geophysical Research, v. 88, p. 569-583.

______, W. H. K. Lee, and R. F. Yerkes, in press, Geology and seismicity of the eastern Red Mountain fault, Ventura County, California: in D. M. Morton and R. F. Yerkes, eds., Recent reverse faulting in the Transverse Ranges, California: U. S. Geological Survey Professional Paper 1339.

APPENDICES

APPENDIX I: Complete List of Wells Used in Maps and Cross-sections

Key to abbreviations: DF, drill floor; GL, ground level; KB, Kelly bushing; OH, original hole; RD, redrilled hole (RD1, first redrill; RD2, second redrill; etc.); RT, rotary table.

Elevations and depths are given in feet.

COMPLETE LIST OF WELLS USED IN MAPS AND CROSS-SECTIONS

Map No.	Operator	Well Name	Elevation	Total Depth
		Sec. 5 - T3N - R24W		
4	McCarthy Oil & Gas	Hobson 1	1971 KB	5515 OH
				5650 RD1
		Sec. 8 - T3N - R24W		
5	Bond Development Corp.	Rincon 1	573 KB	5485
	Cal.-Time	Federal 8-3	619 KB	5015
	Mobil	Hobson A-1	30	4055
		Hobson A-3	58	6651
		Tomson 3	52	3991
		Tomson 6	42 KB	4430
	Santa Fe	Hobson B-2	82	4360 OH
			88 KB	3280 RD1
		B-4	133	3213 OH
			133 DF	5850 RD1
		B-10A	181	4521 OH
			181	4449 RD1
		B-12	276	4485 OH
			278 DF	4270 RD2
		B-13	492	4400 OH
			492 DF	5250 RD1
		B-16	560	4490 OH
			561 KB	4780 RD1
		B-20	401	4713 OH
			401 DF	5003 RD2
		B-21	416	4536 OH
			415 DF	6290 RD1
			415 DF	5070 RD2
		B-23	133	4091
		B-32	385	4005
		B-33	222	3845 OH
			222 DF	5116 RD2
		B-55	85 DF	4424
		C-8	39 DF	3600
6	Shell	Tomson 1	577 DF	9704 OH
			577 DF	8670 RD1
7	Union	Un.-Std.-Hob. A-1	272 RT	6073 OH
			272 RT	9500 RD1
			272 RT	7565 RD2
			272 RT	6685 RD3

Map No.	Operator	Well Name	Elevation	Total Depth
		Sec. 8 - T3N - R24W (cont.)		
8	Union	Un.-Std.-Hob.	711 RT	11,020 OH
		B-1	711 RT	8958 RD1
			711 RT	7353 RD2
		Sec. 9 - T3N - R24W		
9	Amerada Hess	H & S 1	497 KB	4514 OH
			497 KB	6615 RD1
10	Kellerman	Vigus 1		2300
11	Ridge Oil	Fox 1	540 DF	8000
		Sec. 10 - T3N - R24W		
12	Amerada Hess	R. C. 1	1652 KB	4065 OH
			1652 KB	2715 RD1
13	Shell	Hoffman Trust	1462 KB	11,879 OH
		1-10	1462 KB	13,790 RD2
		Sec. 14 - T3N - R24W		
	Santa Fe	Hobson A-12	890	9092
		A-14	1084	7162 OH
			1084	7988 RD1
		A-15	1007	7998
		A-19	1205	8436
		A-20	1205	8262
		A-21	1423 DF	8935
		A-22	1310 DF	8061 OH
			1310 DF	8549 RD1
		A-23	1310 DF	8645
		A-26	733 DF	8160
		A-27	1057 DF	8140
		A-28	915 DF	8658
		A-28-1	901 DF	7957
		A-29	915 DF	8250
		A-30	1423 DF	9034 OH
			1423 DF	8818 RD1
		A-31	1423 DF	9080
		A-37	1057	8390
		Sec. 15 - T3N - R24W		
	Conoco	Hobson 1	381 KB	4824 OH
			381 KB	6390 RD2
			381 KB	6060 RD3
		2	564	5759

Map No.	Operator	Well Name	Elevation	Total Depth
		Sec. 15 - T3N - R24W (cont.)		
15	Conoco	Hobson 3	565 KB	7210
		4	856	6580 OH
			856	6580 RD1
			856 KB	6300 RD2
		5	334 KB	5900 RD2
		6	587 KB	12,194
16	Conoco	Mobil-Padre 1	711 KB	14,100 OH
			711 KB	15,190 RD1
	Mobil	Padre 1	511	6080
		2	895	5650 OH
			895 DF	6270 RD1
		3	512	5900
		4	410	5280 OH
			416 KB	5485 RD4
		6	882 KB	6222
		7	882 KB	5660
		8	882 KB	5610
		9	830 KB	5435
		10	830 KB	5600
		11	830 KB	5300
		12	830 KB	5610
		13	748 KB	6000
		14	748 KB	5510
		16	748 KB	6000
		17	748 KB	5800
		18	782 KB	5650
		19	782	5550 OH
			784 KB	5726 RD1
		20	784 KB	5670
		22	784 KB	6350 OH
			784 KB	5550 RD4
		24	879 KB	6330
		25	879 KB	6269
		26	879 KB	6030 OH
			879 KB	5990 RD1
		28	784 KB	5635
		29	422 KB	5595
		30	421 KB	5205
		50	748 KB	4605
		52	749 KB	5955
		55	748 KB	4577
		56	748 KB	4135
		57	748 KB	4195
		58	748 KB	3915
		59	879 KB	4880

Map No.	Operator	Well Name	Elevation	Total Depth
		Sec. 15 - T3N - R24W (cont.)		
17	Mobil	Padre 61	880 KB	4830 OH
			892 KB	5810 RD1
		70	691 KB	10,483
		100	573 KB	11,667
		101	422 KB	11,208
		102	422 KB	11,265
		103	422 KB	11,162
		104	422 KB	11,386
		105	512 KB	11,764
		106	510 KB	11,670
		107A	880 KB	11,829
17	Mobil	Smith-Hobson 70	596 KB	11,500
	Santa Fe	Hobson A-4-1	536 KB	6740
		A-5	324 DF	5223 OH
			324 DF	6208 RD1
		A-6	360	5425
		A-6-1	360 KB	7687
		A-7	510	6000 OH
			510	6688 RD2
		A-8	593	6905 OH
			593	6910 RD1
		A-8-1	599 KB	7885
		A-9	796 DF	6753 OH
			796 DF	7003 RD1
		A-11	244	7002
		A-35	329 DF	12,300
		A-35-1	335 DF	7905
		A-36	530 DF	12,180
		A-40	334 KB	6300
		A-41	631 KB	6290
18	Shell	Hobson-Smith	591 DF	6275 OH
		2-1	591 DF	6144 RD1
		Sec. 16 - T3N - R24W		
	Santa Fe	Hobson B-1	484	5451 RD1
		B-1-W	508 DF	2751
		B-9	531	6104
		B-9-1	541 DF	10,870
		B-24	354 KB	5067
		B-24-1	349 DF	5325
		B-24-2	349 DF	5110
		B-26	500	4920 OH
			505 DF	6124 RD1
		B-26-1	505	5349

Map No.	Operator	Well Name	Elevation	Total Depth
		Sec. 16 - T3N - R24W (cont.)		
	Santa Fe	Hobson B-27	691	4917 OH
			691	5543 RD4
		B-27-2	695 DF	5516
		B-28	578 DF	6177 RD2
		B-28-2	581 DF	5430
		B-29	679 DF	6321 RD1
		B-29-1	688 DF	10,975
		B-29-2	682 DF	5050
		B-29-3	679 DF	3682
		B-30	742 DF	4900 OH
			742 DF	6765 RD1
		B-30-1	747 DF	11,065
		B-30-3	745	6350
		B-34	562 DF	5050 OH
			562 DF	6329 RD1
		B-35	818	5278 OH
			818	6190 RD2
		B-35-2	820 DF	11,352
		B-35-3	820 DF	11,383
		B-37	551	4805 OH
			551 DF	5200 RD2
		B-37-1	551 DF	6112
		B-39-1	654 DF	5925
		B-40	678	5502
		B-41	202 DF	4837 OH
			202 DF	4703 RD1
		B-43	202	4950 OH
			202	5530 RD1
		B-44		4850 OH
			692 GL	6374 RD1
		B-46	656 DF	5618 OH
			656 DF	6360 RD1
		B-46-1	659 DF	3165 OH
			659 DF	3905 RD1
		B-47	773 DF	5400
		B-47-1	773 DF	3328 OH
			773 DF	5013 RD1
		B-48	345	5119
		B-48-1	345	4767
		B-49	388 DF	5210
		B-51	343	5280
		B-51-1	302 KB	10,784
		B-53	773 DF	5223
		B-54	202 DF	5641
		B-60	298 DF	5379 OH
			300 DF	4750 RD1

Map No.	Operator	Well Name	Elevation	Total Depth
		Sec. 16 - T3N - R24W (cont.)		
	Santa Fe	Hobson B-70	343	5515
		B-72	343 DF	5432
		B-73	343 DF	4740
		B-74	345 DF	5316
		B-75	343 DF	5400
		B-80	368 DF	5995
		B-81	368	4305 OH
			368	5649 RD1
		B-90	279 DF	5510 OH
			279 DF	4800 RD1
		B-100	396 DF	10,926
		B-100-1	398 DF	10,762
		B-102	396 DF	5350
		B-110	660 DF	7055
		B-120	646 DF	5832
		B-121	646 DF	5831
		B-130	528 DF	10,996 RD1
		B-150	848 DF	12,343
		B-150-1	848 DF	6356
		B-162	704 DF	10,800
		B-167	711 DF	10,887
		B-167-1	711 DF	10,977
		B-167-2	713 DF	4020
		Sec. 17 - T3N - R24W		
	Oceanic (Bell)	S. P. 1	28 KB	7650
	Richfield (Arco)	Hobson 5	20 KB	9110
	Richfield (Arco)	Hobson 6	22 KB	9087
	Santa Fe	Hobson B-5	414 DF	5158 OH
			414 DF	4148 RD1
		B-7		7885 OH
			198 DF	4789 RD1
		B-8		5522 OH
			204 DF	5520 RD1
			204 DF	5123 RD2
		B-8-1	210 DF	10,053
		B-14	390	4390 OH
			390	5395 RD1
		B-15-1	453 DF	5295
		B-17-1	191 DF	10,215
		B-18-1	127 DF	4602
		B-18-2	125 DF	4607

Map No.	Operator	Well Name	Elevation	Total Depth
		Sec. 17 - T3N - R24W (cont.)		
	Santa Fe	Hobson B-19	145 DF	4240 OH
			145 DF	5120 RD1
		B-25	310 DF	4657 OH
			310 DF	4555 RD2
		B-25-3	322	5040
		B-31	508 DF	4052 OH
			508 DF	5090 RD1
		B-38	249 DF	3908 OH
			249 DF	5048 RD1
		B-42-1	274 DF	4938
		B-45	296	4987 OH
			300 KB	5300 RD1
		B-58	198 DF	4730
		B-63	198 DF	4540
		B-160	177 DF	11,965
		B-161	427 DF	10,415
		B-163	281 DF	10,405
		B-163-1	281 DF	9943
		C-2	24	3686
		C-3	24	10,515
		C-7	67	3600
		C-9	49 DF	9258 OH
			49 DF	9656 RD3
19		C-10A	35 DF	10,002 OH
			35 DF	11,650 RD2
		C-11	49 DF	14,059
		C-12	44 DF	11,547
		C-13	34 DF	9623
		C-14	49 DF	9521
		C-15	34 DF	8317
		C-16	37 KB	4210
		C-18	39 DF	4247
		C-20	41 DF	4315
		Sec. 21 - T3N - R24W		
20	Arco	Smith-Hoffman 1	55 KB	8107
		Sec. 22 - T3N - R24W		
21	Chevron	St. 3403-1	47 KB	17,000
22	Chevron	S. P. Pitas Point 1	47 KB	9695
23	Conoco	CCMO-Hobson A-1	296 KB	8648 OH
			296 KB	7240 RD1
24	Petrominerals	CWOD-Faria 1	120 KB	7070 RD2

Map No.	Operator	Well Name	Elevation	Total Depth
		Sec. 22 - T3N - R24W (cont.)		
25	Santa Fe	Faria 1	50 KB	14,717
26	Santa Fe	Hobson A-1	222	6970
		Sec. 23 - T3N - R24W		
27	Getty	Valenzuela 1	374	7828
	Santa Fe	Hobson A-2	950	7892 OH
			950	7826 RD3
		A-3	501	4167
		A-10	519	7260 OH
			519	7400 RD1
		A-10-1	519 DF	11,376 OH
			519 DF	6313 RD1
			519 DF	6403 RD2
			519 DF	7839 RD3
			519 DF	7634 RD4
		A-13	805	7568
		A-17	672 DF	7740 RD1
			672 DF	7750 RD2
		A-18	597	7371
		A-25	507 DF	7252
		A-38	980 DF	13,910 OH
			980 DF	11,627 RD1
			980 DF	13,288 RD3
		A-42	463 KB	9210
		A-43	463 KB	13,365 OH
			463 KB	13,366 RD1
		A-44	644 KB	11,780
		A-45	466 KB	13,289
		A-46	664 KB	11,448
		A-47	664 KB	11,540
		A-48	596 KB	11,700
		A-49	892 KB	11,432 OH
			892 KB	12,156 RD1
	Santa Fe	Oak Grove 1	740	7401
		2-1	712 DF	7403
		2-2	707 DF	7296
		2-3	712 DF	7936
		3	901	7230 OH
			901	7124 RD1
		3-2	907 DF	6955
		5-A	591 DF	7797
		7	641	7171 OH
			641 DF	7210 RD1
		7-2	641 DF	7750
		7-3	641 DF	7215

Map No.	Operator	Well Name	Elevation	Total Depth
		Sec. 23 - T3N - R24W (cont.)		
	Santa Fe	Oak Grove 8	656 DF	7233
		9	970 DF	8575
		9-1	966 DF	7700
		9-2	966 DF	5902 OH
			966 DF	8397 RD1
		10	686 KB	11,950
		11	703 KB	11,390
		12	750 KB	13,170
		13	750 KB	9900 OH
			750 KB	10,800 RD1
		Sec. 27 - T3N - R24W		
31	Union	Santa Barbara C. H. 13	22 RT	7086
		Rancho Santa Ana Land Grant		
1	Conoco	Casitas 1		8018
2	Conoco	Casitas 2		12,188
		Rancho Cañada de San Miguelito Land Grant		
28	Chevron	Solimar S. P. C. H. 1	33 DF	6469
	Conoco	Grubb 1	791 KB	7622
		3	742 DF	6625 OH
			742 DF	6455 RD1
			742 DF	6382 RD2
			742 DF	7015 RD3
		20	268 DF	6895 OH
			268 DF	6973 RD1
		28	549 DF	6834 OH
			549 DF	6560 RD1
			549 DF	7583 RD2
		38	1130 DF	9548
		54	514 KB	7250 RD2
29		94	89 KB	11,253
		102	384 KB	11,430
		103	794 KB	12,162
		104	536 GL	13,055
		109	374 KB	11,545
		110	922 KB	12,145 OH
			922 KB	14,116 RD1
		111	1025 KB	12,600
		112	1164 KB	12,710

Map No.	Operator	Well Name	Elevation	Total Depth
	Rancho Cañada de San Miguelito Land Grant (cont.)			
	Conoco	Grubb 114	926 KB	12,359
		115	804 KB	12,046
		139	723 DF	8560 OH
			723 DF	11,050 RD1
		151	921 KB	13,630
		152	923 KB	13,785
		153	731 KB	13,467 OH
			731 KB	14,219 RD1
		154	1022 KB	13,870
		155	278 KB	12,125 OH
			278 KB	13,176 RD1
			278 KB	13,626 RD2
		156	1022 KB	14,609
		157	744 KB	14,094 OH
			744 KB	14,035 RD1
		158	1167 KB	13,616
		159	798 KB	13,900
		160	797 KB	15,878
		161	573 KB	13,750
		162	1022 KB	14,192
		163	1149 KB	15,324
		164	798 KB	14,276
		165	1134 KB	14,586 OH
			1134 KB	14,840 RD1
		166	758 KB	14,200 OH
			758 KB	13,050 RD2
		167	924 KB	8182 OH
			924 KB	14,587 RD1
		168	978 KB	11,811 OH
			978 KB	13,192 RD1
		169	757 KB	7959 OH
			757 KB	14,100 RD1
		170	981 KB	14,717
		171	758 KB	14,907
		172	572 KB	13,785
14		173	937 KB	11,388 OH
			937 KB	12,107 RD1
		180	733 KB	13,941 OH
			733 KB	13,000 RD1
			733 KB	13,175 RD2
			733 KB	12,900 RD3
		181	662 KB	13,433
		182	1101 KB	15,600
		201	1131 KB	14,194
		244	934 DF	8622
		265	729 KB	9540

Map No.	Operator	Well Name	Elevation	Total Depth
	Rancho Cañada de San Miguelito Land Grant (cont.)			
	Conoco	Grubb 278	1105 KB	8273
		301	1042 KB	16,727
		304	847 KB	9428
		309	892 KB	8926
		319	727 KB	9707
		351	885 KB	12,018
		353	1111 KB	13,360 OH
			1111 KB	13,467 RD1
		356	573 KB	12,423
		358	614 KB	13,229
		359	619 KB	12,874
		361	620 KB	14,030
		401	529 DF	7530
		402	372 DF	7150
		403	313 DF	7172
		404	348 KB	7080
		405	656 KB	7838
		406	354 KB	7120
		407	606 KB	7790
		408	645 KB	7488
		409	654 KB	7440
		410	623 KB	7726
		411	797 KB	7635
		412	712 KB	7660 OH
			712 KB	7745 RD1
		413	756 KB	7795
		414	802 KB	8039
		415	1085 KB	12,735 OH
			1085 KB	8435 RD1
			1085 KB	8600 RD2
		416	945 KB	8150
		417	1327 KB	9010
		418	1329 KB	6880 OH
			1329 KB	8777 RD1
		419	867 KB	8214
		420	605 KB	7825
		451	350 KB	9860
		452	654 KB	10,105
		453	723 KB	12,120 OH
			723 KB	9010 RD2
		454	723 KB	9440 OH
			723 KB	9070 RD1
		455	703 KB	13,185 RD1
			703 KB	13,185 RD3
		456	649 KB	9580
		457	1020 KB	9753

Map No.	Operator	Well Name	Elevation	Total Depth
		Rancho Cañada de San Miguelito Land Grant (cont.)		
	Conoco	Grubb 458	529 DF	9410
		459	1019 KB	9730 OH
			1019 KB	7800 RD1
		460	740 DF	9530
		461	1035 KB	9931
		462	740 DF	9660
		463	740 DF	9695
		464	375 DF	9645
		467	649 KB	9618
		501	530 KB	10,344
		502	607 KB	9570
		503	768 KB	9990
		504	567 KB	11,185
		506	536 KB	11,180
		561	611 KB	15,002
		562	537 KB	12,075
		563	910 KB	12,370
		564	1003 KB	12,958
		565	703 KB	13,461
		566	963 KB	13,080
		601	488 KB	10,029
		602	530 KB	11,149
		603	536 KB	11,959
		604	606 KB	10,800
		605	606 KB	11,325
		606	567 KB	11,412
		608	664 KB	11,750 OH
			664 KB	12,059 RD1
		609	989 KB	12,768 OH
			989 KB	14,553 RD1
			989 KB	7210 RD2
		610	988 KB	12,145
		701	486 KB	12,200
		703	539 KB	12,045 OH
			539 KB	13,600 RD1
		704	530 KB	12,788
		705	686 KB	13,175 OH
			686 KB	13,150 RD2
			686 KB	13,300 RD3
		706	683 KB	13,340
		707	681 KB	12,765
		708	610 KB	13,440
		709	768 KB	12,768
		801	962 KB	14,295
		802	610 KB	13,900
		803	640 KB	13,110

Map No.	Operator	Well Name	Elevation	Total Depth
	Rancho Cañada de San Miguelito Land Grant (cont.)			
	Conoco	Grubb 804	703 KB	13,896
30	Pauley Petroleum	C. H. 8-26-3A	32 KB	7724
	Shell	Taylor 335	431 DF	9060 OH
			431 DF	10,919 RD1
		410	772 DF	11,750
		421	505 DF	11,700
		438	821 DF	11,554
		440	521 DF	12,850
		445	779 DF	12,697
		453	807 DF	10,640
		469	807 DF	12,985
		484	666 DF	13,315
3	Shell	Wood 1		5745
	Offshore			
32	Chevron	C. H. 8R-49	17 KB	4519
33	Pauley Petroleum	C. H. 8-22-1A	12 KB	5520
34	Pauley Petroleum	C. H. 8-22-2A	20 KB	4508

APPENDIX II: Plates I - XVII

(In pocket)